

# A palaeogenomic investigation of overharvest implications in an endemic wild reindeer subspecies

Fabian L. Kellner<sup>1,2</sup>  | Mathilde Le Moullec<sup>2,3</sup>  | Martin R. Ellegaard<sup>1</sup>  |  
 Jørgen Rosvold<sup>4</sup>  | Bart Peeters<sup>2</sup>  | Hamish A. Burnett<sup>1,2</sup>  |  
 Åshild Ønvik Pedersen<sup>5</sup>  | Jaelle C. Brealey<sup>1</sup>  | Nicolas Dussex<sup>1</sup>  |  
 Vanessa C. Bieker<sup>1</sup>  | Brage B. Hansen<sup>2,6</sup>  | Michael D. Martin<sup>1,2</sup> 

<sup>1</sup>Department of Natural History, NTNU University Museum, Norwegian University of Science and Technology (NTNU), Trondheim, Norway

<sup>2</sup>Centre for Biodiversity Dynamics, Department of Biology, Norwegian University of Science and Technology (NTNU), Trondheim, Norway

<sup>3</sup>Department of Mammals and Birds, Greenland Institute of Natural Resources (GINR), Nuuk, Greenland

<sup>4</sup>Department of Terrestrial Biodiversity, Norwegian Institute for Nature Research (NINA), Trondheim, Norway

<sup>5</sup>Norwegian Polar Institute, Fram Centre, Tromsø, Norway

<sup>6</sup>Department of Terrestrial Ecology, Norwegian Institute for Nature Research (NINA), Trondheim, Norway

## Correspondence

Fabian L. Kellner and Michael D. Martin, Department of Natural History, Norwegian University of Science and Technology, University Museum, Erling Skakkes Gate 47A, Trondheim 7012, Norway.

Email: [fabian.l.kellner@ntnu.no](mailto:fabian.l.kellner@ntnu.no) and [mike.martin@ntnu.no](mailto:mike.martin@ntnu.no)

Mathilde Le Moullec, Department of Birds and Mammals, Greenland Institute of Natural Resources (GINR), Nuuk, Greenland.

Email: [malm@natur.gl](mailto:malm@natur.gl)

## Funding information

Svalbard Environmental Protection Fund, Grant/Award Number: 14/137 and 15/105; Norwegian Research Council, Grant/Award Number: 223257, 276080 and 325589; Arctic Field Grant, Grant/Award Number: 235652, 246054 and 257173

**Handling Editor:** Brent Emerson

[Correction added on 23 February 2024, after first online publication: The copyright line was changed.]

## Abstract

Overharvest can severely reduce the abundance and distribution of a species and thereby impact its genetic diversity and threaten its future viability. Overharvest remains an ongoing issue for Arctic mammals, which due to climate change now also confront one of the fastest changing environments on Earth. The high-arctic Svalbard reindeer (*Rangifer tarandus platyrhynchus*), endemic to Svalbard, experienced a harvest-induced demographic bottleneck that occurred during the 17–20th centuries. Here, we investigate changes in genetic diversity, population structure, and gene-specific differentiation during and after this overharvesting event. Using whole-genome shotgun sequencing, we generated the first ancient and historical nuclear ( $n=11$ ) and mitochondrial ( $n=18$ ) genomes from Svalbard reindeer (up to 4000 BP) and integrated these data with a large collection of modern genome sequences ( $n=90$ ) to infer temporal changes. We show that hunting resulted in major genetic changes and restructuring in reindeer populations. Near-extirpation followed by pronounced genetic drift has altered the allele frequencies of important genes contributing to diverse biological functions. Median heterozygosity was reduced by 26%, while the mitochondrial genetic diversity was reduced only to a limited extent, likely due to already low pre-harvest diversity and a complex post-harvest recolonization process. Such genomic erosion and genetic isolation of populations due to past anthropogenic disturbance will likely play a major role in metapopulation dynamics (i.e., extirpation,

Fabian L. Kellner and Mathilde Le Moullec contributed equally.

Vanessa C. Bieker, Brage B. Hansen, Michael D. Martin contributed to research supervision.

This is an open access article under the terms of the [Creative Commons Attribution](#) License, which permits use, distribution and reproduction in any medium, provided the original work is properly cited.

© 2024 The Authors. *Molecular Ecology* published by John Wiley & Sons Ltd.

recolonization) under further climate change. Our results from a high-arctic case study therefore emphasize the need to understand the long-term interplay of past, current, and future stressors in wildlife conservation.

#### KEY WORDS

ancient DNA, bottleneck, conservation genomics, genomic erosion, population genomics, Svalbard reindeer

## 1 | INTRODUCTION

Excessive harvest reduces population size and genetic diversity and can ultimately lead to local extirpation or global (i.e., species) extinction (Frankham, 2005; Spielman et al., 2004). Overharvesting, also called overexploitation, has long impacted fish and large mammals and occurs today in combination with additional risk of climate change and habitat loss (Bowyer et al., 2019; IUCN, 2020; Lorenzen et al., 2011; Luypaert et al., 2020). Populations may recover demographically after overharvest and near-extinction events, but their genetic diversity can remain low (Lande et al., 2003). Harvest-induced bottlenecks will likely also reduce a species' resilience and adaptive capabilities when facing future challenges such as global climate change (Frankham et al., 2002). Nevertheless, despite that genetic diversity, along with species and ecosystem diversity, is recognized as one of the three pillars of biodiversity, it is not yet widely considered by conservation policymakers (Jensen et al., 2022; Laikre et al., 2010). It is therefore important to quantify the loss of genetic variation and changes in population genetic structure following such bottlenecks, in order to appropriately set conservation measures and to better predict the trajectory of the potential recovery.

Contemporary genetic material can hold considerable information about past demographic processes. For instance, methods employing coalescent theory can retrospectively detect genetic bottlenecks and inform on their magnitude and timing (Drummond et al., 2005). However, information about lineages that went extinct during the bottleneck is lost. Therefore, investigation of effects of past bottlenecks like overharvesting from only contemporary material may overlook the severity of the event (Leonardi et al., 2017). Advances in the fields of genomics and ancient DNA (aDNA) enable population-level whole-genome sequencing of nuclear and mitochondrial genomes, for instance, of specimens living prior to harvest-induced bottlenecks (Leonardi et al., 2017; Mitchell & Rawlence, 2021). Ancient DNA is therefore a powerful tool that allows for direct temporal comparisons, setting a 'baseline' for the state of the species before anthropogenic intrusions (Díez-Del-Molino et al., 2018; Jensen et al., 2022). The respective measures of genetic change through time are valuable in ecological, evolutionary, and conservation contexts, with a potential to inform future conservation efforts (Jensen et al., 2022), for example, by studying genomic erosion (Robin et al., 2022; Sánchez-Barreiro et al., 2021), the sum of genetic threats to small populations, such as decreasing genome-wide diversity, increasing genetic load and inbreeding, and reducing genome-wide heterozygosity (Díez-Del-Molino

et al., 2018; Frankham, 2005; Kohn et al., 2006). By comparing the genomes of different temporal populations, regions of high genomic divergence can be identified. Genes within these regions likely experienced evolution due to selection or genetic drift (Allendorf & Hard, 2009; Therkildsen et al., 2019).

Because wildlife extirpations (i.e., local population extinctions) are expected to accelerate in the future (IUCN, 2020), knowledge of past genetic changes is crucial to predict the future population genetics of populations that are currently in decline due to harvesting, climate change, habitat loss, or competition with invasive species. Many Arctic mammals, such as bowhead whale (*Balaena mysticetus*, Linnaeus, 1758) and walrus (*Odobenus rosmarus*, Linnaeus, 1758), as well as some reindeer and caribou (*Rangifer tarandus*, Linnaeus, 1758) subspecies, experienced large-scale local extirpations about a century ago (CAFF, 2013). Some of the subspecies, for example, the Dawson caribou (*R. t. dawsoni* (Seton, 1900)) from Haida Gwaii off the coast of Canada and the East Greenland caribou (*R. t. eogroenlandicus*, Degerbøl, 1957), were even driven to extinction (Byun et al., 2002; Gravlund et al., 1998).

The wild Svalbard reindeer (*Rangifer tarandus platyrhynchus*, Vrolik, 1829), a subspecies endemic to the Svalbard archipelago with distinct morphological and behavioural characteristics, was hunted down to approximately 1000 individuals and extirpated from ~60% of its range before being protected by law in 1925 (Lønø, 1959). The reindeer survived in four remote locations (populations), from which they then slowly recolonized the archipelago, partially assisted by two translocation programs (Aanes et al., 2000), to reach a current population size of ~22,000 individuals (Le Moullec et al., 2019). Conveniently, the cold and dry Arctic environment physically preserves ancient skeletal material and its genetic information to a relatively high degree. Ancient DNA from bones and antlers from Svalbard reindeer that lived prior to the presence of humans (before the 17th century) therefore represent a unique opportunity to quantify effects of harvest-induced bottlenecks on the genetic composition of present-day metapopulations (Le Moullec et al., 2019). Thus, by comparing contemporary DNA with ancient DNA from Svalbard reindeer, this 'natural experiment' can provide valuable information on the genetic consequences of harvest-induced bottlenecks and population recovery following successful conservation efforts in large animals.

Reindeer most likely colonized Svalbard from Eurasia through intermediate colonization of the Franz Josef Land archipelago as a stepping-stone (Kvie et al., 2016). The earliest published subfossil evidence of reindeer presence on Svalbard was dated to 5000–3800 BP (van der Knaap, 1989), but there is both molecular (Dussex

et al., 2023) and radiocarbon dating evidence (Le Moullec, Martin and Hansen, unpubl. dating of an antler) that the colonization of Svalbard started earlier at around 8000–6000 BP (Dussex et al., 2023). The locations of a sample of carbon-dated ancient bones suggest they subsequently spread across the entire Svalbard archipelago (Le Moullec et al., 2019; van der Knaap, 1989). Harvest began when Svalbard was discovered in 1596, but the most intensive hunting period of reindeer occurred in the early 1900s (Hoel, 1916; Lønø, 1959; Wollebaek, 1926), until protection in 1925. Lønø (1959) documented that reindeer had then survived at low abundance in Nordenskiöld Land (central Spitsbergen), Reinsdyrflya (North Spitsbergen), Nordaustlandet (North East Svalbard), and Edgeøya (East Svalbard). Since then, reindeer have recolonized most of their former range from these four remnant populations (Peeters et al., 2020).

Six genetically distinct reindeer groups are now present on the Svalbard archipelago: four populations that expanded from their respective 'hunting refugia', and two populations founded by individuals from central Spitsbergen. Of the latter, one was founded along the west coast of Spitsbergen following two translocations, and another was founded by natural recolonization to south Spitsbergen, with strong genetic drift following gradual expansion (Burnett et al., 2023; Peeters et al., 2020). Svalbard reindeer disperse slowly due to their sedentary behaviour and the fragmented landscape (Le Moullec et al., 2019). Habitat connectivity is further reduced with climate warming and declining cover of coastal sea ice, which provides an important dispersal corridor (Peeters et al., 2020). Because hunting, predation, insect harassment, and intra-specific competition for resources play only minor roles today (Derocher et al., 2000; Reimers, 1984; Stempniewicz et al., 2021; Williamsen et al., 2019), population growth is mainly determined by the density-dependent weather effects on access to resources in winter (Albon et al., 2017; Hansen et al., 2019; Loe et al., 2020).

While some wild reindeer/caribou subspecies are undergoing strong declines due to anthropogenic landscape fragmentation and climate change (Collard et al., 2020; Festa-Bianchet et al., 2011), the Svalbard reindeer is increasing in abundance (Hansen et al., 2019; Le Moullec et al., 2019). This increase is mainly driven by recovery from the past overharvesting and by climate change improving and enhancing the length of snow-free season (Hansen et al., 2019; Le Moullec et al., 2019; Loe et al., 2020). The Svalbard reindeer genetic diversity is by far the lowest among the *Rangifer* subspecies (Dussex et al., 2023; Kvie et al., 2016; Yannic et al., 2013). Despite this, local variation in genetic diversity is strong, with decreasing diversity from central Spitsbergen towards the peripheries of the archipelago (Burnett et al., 2023; Kvie et al., 2016; Peeters et al., 2020). Inbreeding (i.e., long runs of homozygosity) is stronger in the non-admixed naturally recolonized populations than in the two translocated populations, likely as a result of having experienced a series of bottlenecks (Burnett et al., 2023). The translocated populations largely maintained the genetic diversity level of their source populations, despite <15 founder individuals for each translocation, likely because of rapid population growth and overlapping generations (Burnett et al., 2023).

Here, we investigate the genetic impacts of the population bottleneck caused by the past overharvest of Svalbard reindeer. We hypothesize that the reindeer suffered genomic erosion due to this overexploitation event. To infer changes in genetic structure, diversity, and allele frequencies, we integrated palaeogenomic data with a large dataset of contemporary genome sequences and estimated genetic diversity and genomic erosion before (4000–400 calibrated years Before Present [BP]), during (500–0 BP, equating to 1500–1950 Common era [CE], also corresponding to the period with uncertain carbon-dating) and after the overharvesting period (>1950 CE).

## 2 | MATERIALS AND METHODS

### 2.1 | Study system and sample acquisition

The Svalbard archipelago (76°–81°N, 10°–35°E) is surrounded by the Greenland and Barents Seas, south of the Arctic Ocean. The archipelago consists of over 500 islands, the largest being Spitsbergen, Nordaustlandet, Edgeøya, Barentsøya, and Prins Karls Forland. Reindeer inhabit vegetated land patches, which make up only 16% of the land cover, fragmented by fjords and tidewater glaciers (Johansen et al., 2012). Central Spitsbergen and Edgeøya hold a network of unglaciated valleys with the highest density of reindeer (Le Moullec et al., 2019).

At the time of the oldest evidence of reindeer on Svalbard (~5000 BP), the Svalbard summer climate was approximately 1.5–2°C warmer than the recent reference period of 1912–2012 CE (van der Bilt et al., 2019). The climate became progressively cooler over time until the pre-industrial period at around 1500 CE (van der Bilt et al., 2019), with increasing sea-ice cover in the Fram Strait (Werner et al., 2016). Currently, Svalbard is among the regions on Earth experiencing the strongest temperature increase, with 0.5°C increase per decade in summer and 1.3°C increase per decade for year-round measurements at Svalbard Airport, 2001–2020 CE (Isaksen et al., 2022). Partly related to this, the sea-ice concentration around Svalbard has decreased drastically in recent years at a rate of 10%–15% per decade in winter, 2001–2020 CE (Isaksen et al., 2022). The West side of Spitsbergen is now ice-free year-round, except for some inner fjords or in front of some tidewater glaciers.

Subfossil bones and antlers ( $n=18$ ) were collected from various sites across the Svalbard archipelago during 2014–2015 CE as described previously (Le Moullec et al., 2019) with approval by the Governor of Svalbard (RIS-ID: 10015 and 10128). Two subfossils originating from Franz Joseph Land, collected in 2007, were used as an outgroup in the mitochondrial haplotype network and followed the same laboratory procedure as the ancient Svalbard subfossils. Sample ages were determined via  $^{14}\text{C}$  dating (Table 1). All  $^{14}\text{C}$  dates were calibrated with the IntCal20 calibration curve (Reimer, 2020) using the *calibrate* function in the package *rcarbon* (Crema & Bevan, 2021) in R v4.1.0 (R Core Team, 2021). The subfossil materials were combined with a previously published genomic dataset from samples collected in 2014–2018 and consisting of 90

TABLE 1 Ancient Svalbard reindeer sample overview. Sample provenance ('E'=East, 'C'=central) indicated with their UTM East and UTM North coordinates. Reported ages are calibrated radio-carbon-dated ages (IntCal20) in calendar years before present (BP, before 1950 CE). Summary of sample and mean mapping depths of ancient nuclear genomes (nDNA) against the Svalbard reindeer and caribou reference genome, as well as the reindeer mitochondrial (mtDNA) reference genome. Sample provenance, sequencing, and mapping statistics of ancient samples against the Svalbard reindeer reference genome.

ID	Area	UTM-E	UTM-N	Median age (BP)	Age range (BP, 2 sigma)	Hunting period	Svalbard reference nDNA	Caribou reference nDNA	Reindeer reference mtDNA	Analyses included
B20	E-Svalbard	651368	8661900	2351	2329-2460 <sup>b</sup>	Pre	0.02	0.02	956	mtDNA
BBH7	Nordaustlandet	644458	8915138	511	500-521 <sup>b,c</sup>	Pre	3.72	3.66	386	nDNA mtDNA
M44	C-Spitsbergen	536291	8707272	597	525-644 <sup>a</sup>	Pre	6.78	6.67	534	nDNA mtDNA
M46	C-Spitsbergen	536023	8706959	703	668-768 <sup>a</sup>	Pre	2.65	2.60	442	nDNA mtDNA
M68	C-Spitsbergen	545390	8700500	NA	0-447 <sup>a</sup>	During	3.99	3.93	211	nDNA mtDNA
M72	C-Spitsbergen	546200	8701580	958	916-1057 <sup>a</sup>	Pre	0.03	0.03	90	mtDNA
MB60	E-Svalbard	637956	8689040	NA	27-260 <sup>b</sup>	During	1.52	1.50	284	nDNA mtDNA
MDV11	E-Svalbard	633986	8688774	605	549-647 <sup>b</sup>	Pre	4.55	4.49	1870	nDNA mtDNA
MLM12	E-Svalbard	651249	8661821	1326	1298-1349 <sup>b</sup>	Pre	0.02	0.02	30	mtDNA
MLM16	E-Svalbard	651084	8661716	1762	1716-1821 <sup>b</sup>	Pre	0.04	0.04	118	mtDNA
MLM51	E-Svalbard	655011	8650398	1968	1894-2046 <sup>b</sup>	Pre	0.07	0.07	243	mtDNA
MLM61	E-Svalbard	637640	8688976	1875	1825-1935 <sup>b</sup>	Pre	0.57	0.20	33	nDNA mtDNA
MLM80	E-Svalbard	655480	8700183	3912	3846-3973 <sup>b</sup>	Pre	0.02	0.02	205	mtDNA
MLM82	E-Svalbard	655632	8700166	3127	3063-3212 <sup>b</sup>	Pre	0.03	0.02	192	mtDNA
R20	Wijdfjorden	525246	8785449	NA	0-450 <sup>b</sup>	During	12.22	12.14	214	nDNA mtDNA
R25a	Wijdfjorden	525722	8783391	NA	8-277 <sup>b</sup>	During	4.19	4.13	411	nDNA mtDNA
R29a	Wijdfjorden	525722	8783391	NA	12-267 <sup>b</sup>	During	0.73	0.72	57	nDNA mtDNA
R36	Wijdfjorden	525768	8783368	NA	1-282 <sup>b</sup>	During	3.96	3.91	135	nDNA mtDNA

<sup>a</sup>Dated at the Uppsala Angström Laboratory.

<sup>b</sup>Dated at the Norwegian University of Science and Technology, The National Laboratory of Age Determination.

<sup>c</sup>Radiocarbon date from previous study (Le Moullec et al., 2019).

contemporary Svalbard reindeer from a recent population genomics study (PRJEB57293, Burnett et al., 2023). To put harvest-induced changes within Svalbard reindeer populations into a temporal context, we subdivided the samples into three time periods (Figure 1): before (4000–400 years before present [BP], hereafter referred to as *pre-hunting*), during (400 years BP–1950 Common Era, CE, hereafter referred to as *during-hunting*), and after (>1950CE, hereafter referred to as *post-hunting*) the major harvest-induced bottleneck that occurred from the 17th century to the early 20th century (Lønø, 1959).

## 2.2 | DNA extraction, library building, and sequencing

All pre-PCR manipulations of sample genetic material were conducted in a dedicated, positively pressurized ancient DNA laboratory facility at the NTNU University Museum. 48–360mg of bone material were collected using a Dremel disc drill and subsequently crushed to fragments of maximum 1-mm diameter. DNA was extracted with a custom, silica-based extraction protocol. For digestion, a custom digestion buffer consisting of 1.25% (v/v) proteinase K (20mg/mL), 90% (v/v) EDTA (0.5M), and 8.75% (v/v) molecular-grade water was used. Samples were pre-digested in 1mL digestion buffer for 10min at 37°C on a rotor. The samples were spun down, the pre-digest was removed, and 4mL of digestion buffer was added to the samples. Samples were left for digestion on a rotor for 18h at 37°C. The lysis buffer was mixed 1:10 with Qiagen PB buffer modified by adding 9mL sodium acetate (5M) and 2mL NaCl (5M) to a 500mL stock solution. pH was adjusted to 4.0 using concentrated (37%/12M) HCl. 50µL in-solution silica beads were added, and samples were left on

a rotor for 1h at ambient temperature to allow binding of the DNA. Silica pellets with bound DNA were purified using Qiagen MinElute purification kit following the manufacturer's instructions and eluted in 65µL Qiagen EB buffer. For every extraction batch, an extraction blank was carried out alongside the samples.

For each sample and the extraction blanks, 32µL of DNA extract were built into double-stranded libraries. Libraries were prepared following the BEST 2.0 double-stranded library protocol (Carøe et al., 2018). Three DNA extraction blanks were included, as well as a single library blank (no-template control). 10µL of each library were amplified in 50µL reactions with AmpliTaq Gold polymerase, using between 13 and 22cycles and a dual indexing approach (Kircher et al., 2012). The optimal number of PCR cycles for each library was determined via qPCR on a QuantStudio3 instrument (ThermoFisher). The indexed libraries were purified using SPRI beads (Rohland & Reich, 2012) and eluted in 30µL EBT buffer. The amplified libraries were quantified on 4200 TapeStation instrument (Agilent Technologies) using High Sensitivity D1000 ScreenTapes. The libraries were then pooled in equimolar concentrations and initially sequenced on the Illumina MiSeq platform in order to quantify their complexity and endogenous DNA content. The libraries were subsequently subjected to several rounds of PE 150 bp sequencing on the Illumina NovaSeq 6000 platform (Norwegian National Sequencing Centre and Novogene UK).

## 2.3 | Bioinformatic analysis and post-mortem DNA damage assessment

Sequence data from the pooled libraries were demultiplexed according to their unique P5/P7 index barcode combinations. Prior

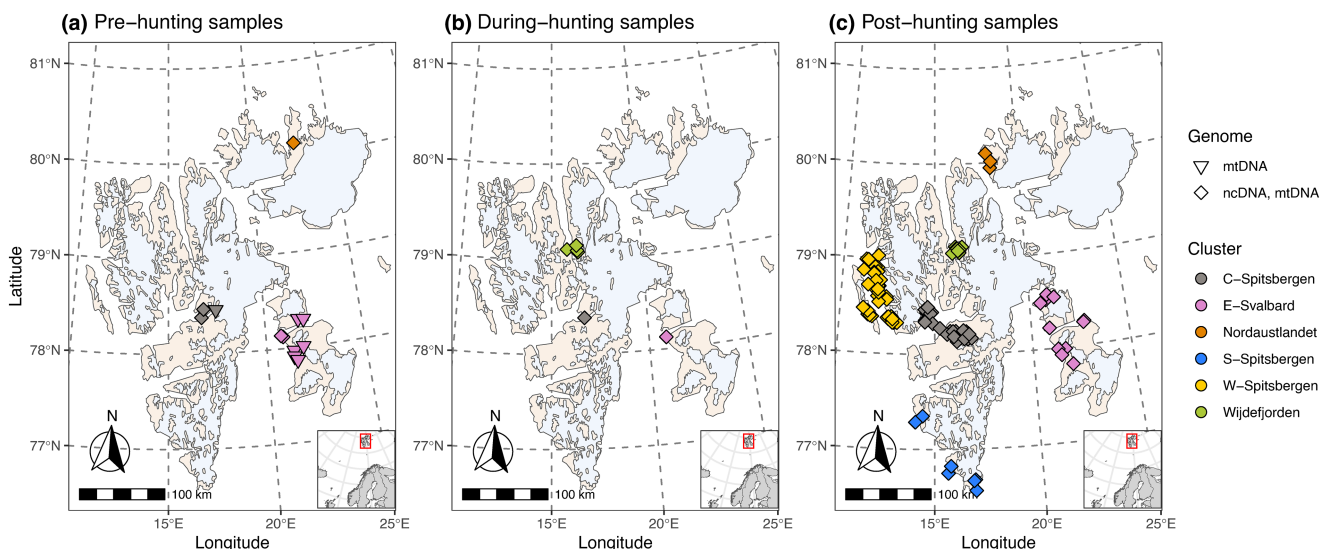


**FIGURE 1** Sampling locations on Svalbard. Glaciated areas are coloured in light blue. Each point symbolizes one individual reindeer. Samples are coloured by affiliation with a geographic cluster. Shape denotes which of the sample's genome sequences were used in this study (ncDNA, nuclear DNA; mtDNA, mitochondrial DNA). Samples were carbon-dated and divided into three time periods. (a) before the hunting period (4000–400 BP), (b) during the hunting period (400 BP–1950CE), and (c) after the hunting period (>1950CE). Points are slightly jittered to reduce overplotting. [Colour figure can be viewed at [wileyonlinelibrary.com](https://wileyonlinelibrary.com)]

to mapping, residual adapter sequences were removed and reads shorter than 25 bases were discarded with AdapterRemoval v2.2.4. Raw reads were mapped initially against the caribou (*Rangifer tarandus caribou*) nuclear genome (Taylor et al., 2019) and the reindeer (*Rangifer tarandus tarandus*) mitochondrial genome (Li et al., 2017) in the framework of the PALEOMIX pipeline v1.2.13.2 (Schubert et al., 2014) using the 'mem' algorithm of the Burrows–Wheeler Aligner (BWA) v0.7.16a (Li, 2013) and no mapping quality (MAPQ) score filtering. PCR duplicates were marked using picard tools v2.20.2 ('Picard Toolkit', 2019) tool MarkDuplicates. Mapped reads were realigned with the Genome Analysis Tool Kit (GATK v3.80) indel realigner (McKenna et al., 2010). Following mapping, soft-clipped reads were removed with samtools v1.12 (H. Li et al., 2009). Then mapDamage v2.0.9 (Jónsson et al., 2013) was used to assess and plot ancient DNA damage patterns and to rescale base quality scores accordingly. Sequencing depth statistics were estimated with samtools depths at a minimum phred-scaled mapping quality of 30 (Table S1). All samples were sequenced to a minimum of 0.2x sequencing depth of the caribou nuclear genome assembly after read filtering.

## 2.4 | Construction of a consensus Svalbard reindeer reference genome

In order to improve mapping rate and more accurately reflect the divergent genome of the Svalbard reindeer, a reference Svalbard reindeer nuclear genome was generated from the deepest sequenced contemporary individuals of each metapopulation (T-15, C7, and B2, see Table S1). BAM files were downsampled to 26.9x, the lowest depth among the three genomes, with the samtools v1.12 view command using the flags -b and -s. Individual bam files were combined into a single bam file. The new reference sequence was determined with angsd v0.931 (Korneliussen et al., 2014) using the -doFasta 2 tool with the options -doCounts 1, -explode 1, -setMinDepthInd 2, -remove\_bads 1, requiring a minimum read mapping quality of 30 and a minimum base quality of 20. All samples were mapped against this new reference genome using the same methods described above.

## 2.5 | Determination of ancestral states

Ancestral states were inferred by mapping publicly available sequencing data from three closely related (Heckeberg & Wörheide, 2019) species (moose, *Alces*, bioproject: PRJEB40679 (Dussex et al., 2020); red deer, *Cervus elaphus*, bioproject: PRJNA324173 (Bana et al., 2018); white-tailed deer, *Odocoileus virginianus*, NCBI PRJNA420098; Accession No. JAAVWD000000000) against the caribou reference genome (Taylor et al., 2019). BAM files were downsampled to 12.3x, the lowest depth among the three genomes, with samtools v1.12 and merged into a single BAM file for all three species. The ancestral state was inferred by choosing the most common base at each

site with angsd v0.931 using the -doFasta 2 tool with the options -doCounts 1, -explode 1, -remove\_bads 1, and -uniqueOnly 1, requiring a minimum read mapping quality of 30 and a minimum base quality of 20.

## 2.6 | Selection of nuclear genomic loci for further analysis

Genomic positions suitable for further downstream analysis were computed for ancient and modern samples with the GATK v3.8-0 CallableLoci tool, requiring a minimum read mapping quality of 30 and a minimum base quality of 20. The input BAM files for the ancient individuals were generated by merging all of that group's BAM files with samtools merge and replacing the read groups with the picard-tools v2.20.2 AddOrReplaceReadGroups tool. For modern samples, only a single BAM file (sample T-15) was used. The average depth of these merged BAM files was calculated with samtools depth at mapping quality 30 and base quality 20 (ancient=43.6, modern=57.4). The minimum depth was calculated as one-third of the mean depth (ancient=15, modern=20) and the maximum depth as twice the mean depth (ancient=87, modern=115). The files were then further processed with bedtools v2.30.0 (Quinlan, 2014) in order to be used with the -sites and -rf options of angsd v0.931. Sites that were marked with excessive coverage or poor mapping quality were excluded from downstream analysis.

## 2.7 | Mitogenome alignment and haplotype analysis

Variants in the mitogenome were identified with GATK v4.2.5.0 using a reindeer mitochondrial genome sequence (Li et al., 2017) as the reference. For this, haplotypes were called with GATK HaplotypeCaller requiring a minimum read mapping quality of 30. Variants were only called when they were above a minimum phred-scaled confidence threshold of 30 (-stand-call-conf 30). We verified that all samples' mitochondrial genomes were sequenced to a minimum depth of 30x after removing reads with mapping quality below 30 (see Table 1). GVCF files were merged using the GATK GenomicsDBImport tool, and a joined SNP call was performed with GATK GenotypeGVCFs with the setting -stand-call-conf 30. Mitochondrial haplotypes in the output variant call format (VCF) file were used to populate a FASTA multiple sequence alignment file using a custom python2 script. In this alignment, insertions and deletions were ignored, and individual haplotypes were deemed ambiguous ('N') if the sequencing depth was <10 reads or if the genotype quality score was <20. Despite these measures, one sample (MB16 with 17% 'N') was ambiguously assigned to a haplotype and therefore removed from the analysis.

We used the *ape* package (Paradis & Schliep, 2019) in R to import the 16,362-bp mitogenome sequence alignment and then extracted haplotypes with the *haplotype* function from the *pegas* package

(Paradis, 2010). We visualized haplotype diversity with a network linking haplotypes based on a parsimony criterion minimizing the number of sites segregating between haplotypes (i.e., TCS algorithm). Such an algorithm uses an infinite site model to calculate a pairwise distance matrix of the haplotypes, with pairwise deletion of missing data. With the haploNet function (Templeton et al., 1992) from *pegas*, we plotted haplotype networks from individuals living before, during, and after the hunting period. Note that for this specific analysis, we included the two mitogenomes from Franz Joseph Land as outgroups to inform on the ancestral Svalbard reindeer haplotype. Across all Svalbard mitogenome sequences and within each time period, we calculated genetic diversity statistics in *pegas*, using the *haplo.div* function to calculate haplotype diversity (Nei & Tajima, 1981) and the *nuc.div* function to calculate nucleotide diversity (Nei, 1987). The number of segregating sites was summed from the *seg.sites* function in *ape*.

## 2.8 | Genotype likelihood estimation

Genotype likelihoods for nuclear genome loci were estimated with *angsd* v0.931, excluding reads with multiple matches to the reference genome (option *-uniqueOnly* 1). Allele frequencies were estimated with the option *-doGlf* 2 using the combined estimators for fixed major and minor allele frequency as well as fixed major and unknown minor allele frequency (*-doMaf* 3). Major and minor allele frequencies were inferred from genotype likelihood data (*-doMajorMinor* 1). Variant sites were considered when they had a minimum minor allele frequency of 5% and minimum number of informative individuals set to half the total number of individuals (*-minInd* 50). Reads with a phred-scaled mapping quality score below 30 were excluded, as were bases with a quality score below 20 as well as reads with a samtools flag above 255 (not primary, failure, and duplicate reads) with the option *-remove\_bads* 1. The first five bases were trimmed from both ends of reads (*-trim* 5), and the frequencies of the bases were recorded with *-doCounts* 1. The depth of each individual (*-dumpCounts* 2) and the distribution of sequencing depths (*-doDepth* 1) were recorded. Files to be used in subsequent analyses with Plink were generated (*-doPlink* 2). Genotypes were encoded (*-doGeno* 2) for downstream analysis. Posterior genotype probabilities were estimated based on allele frequencies as prior (*-doPost* 1). Genotypes were only considered if their posterior probability was above 95% (*-postCutoff* 0.95). Genotypes were considered missing in cases when the individual depth was below 2 (*-geno\_minDepth* 2). Before further analysis, sites in strong linkage disequilibrium were pruned with Plink v1.90 beta 6.24 (Chang et al., 2015) using a window size of 50 kbp, a step size of 3 kbp, and a pairwise  $r^2$  threshold of 0.5 (*-indep-pairwise* 50 3 0.5). Subsequently, regions with low mapping quality, excessive coverage as identified with *CallableLoci* (see above), or associated with sex chromosomes (for methods see Burnett et al., 2023) were removed via a custom python script. Also excluded were sites that are not variant in both the ancient and modern datasets.

## 2.9 | Principal components and admixture analyses

We visually identified related clusters with covariance matrices for principal component analysis (PCA) using PCAngsd v1.10 (Meisner & Albrechtsen, 2018), running 10,000 iterations to ensure convergence. Samples were grouped both spatially and by time period (pre-, during-, and post-hunting). A spatial group was defined as all individuals from each time period that were sampled within 80 km around centroid points calculated by hierarchical clustering with the *Geosphere* package in R (see map in Figure 3b-d and Figures S7-S15). Genetic structure was estimated with NGSadmin (Skotte et al., 2013), including only variant sites with a minimum minor allele frequency of 5% and minimum number of informative individuals set to half the total number of individuals (*-minInd* 50). The number of estimated ancestral populations K ranged from 2 to 10. For each value of K, each of ten replicates was run with different random starting seeds, and the replicate with the highest likelihood was used for plotting. An optimal value for K was estimated with the delta-K method (Evanno et al., 2005). Admixture diversity scores were calculated based on K = 4 using the R package *entropy*, as described in Kim and Harismendy (2017). In order to evaluate possible sampling bias, we repeated the analysis with a reduced dataset (see below).

## 2.10 | Estimation of heterozygosity

Site allele frequency likelihoods were calculated for each sample individually with *angsd* (command-line option *-doSaf* 1) with a minimum base quality of 20 and a minimum read mapping quality of 30, using only selected sites and regions described previously and removing transitions (command-line option *-noTrans* 1) as well as 5 bp from the ends of all reads (*-trim* 5) to reduce artefacts of ancient DNA damage. Reads with multiple best hits and non-primary, failed, and duplicate reads were removed from the analysis (command-line options *-uniqueOnly* 1 and *-remove\_bads* 1). To polarize the site allele frequency (SAF) likelihoods, a FASTA format file with ancestral states (see above) was supplied (command-line option *-anc*). The GATK model (command-line option *-GL* 2) was used to estimate genotype likelihoods. Then, the site frequency spectrum (SFS) was estimated with *angsd* *realSFS* based on the polarized SAF likelihoods. Heterozygosity was then calculated in R as described in the *angsd* documentation. A pairwise Mann-Whitney U test with default settings as implemented in R was performed to judge the significance of differences in heterozygosity between groups. We obtained the delta estimator (Díez-Del-Molino et al., 2018) of heterozygosity ( $\Delta H$ ) by calculating  $\Delta H = \frac{\text{med}(H_2) - \text{med}(H_1)}{\text{med}(H_1)}$ , with  $H_2$  being the set of individual genome-wide heterozygosity values in the younger sample set,  $H_1$  being the set of individual genome-wide heterozygosity values in the older sample set, and med being the median value. The heterozygosity analyses' power ( $1-\beta$ ) was investigated with a one-tailed, two-sample t-test using function *pwr.t2n-test* within the R

package pwr. We removed sample T-26 from the analysis of heterozygosity as its low sequencing depth below 0.5x produced unreliable estimates of heterozygosity multiple orders of magnitude below all other samples.

## 2.11 | Temporal genomic differentiation

To assess the potential phenotypic impacts of overharvest on Svalbard reindeer, we identified genomic regions that were highly differentiated in a comparison of the three time groups among each other. To reduce potential biases introduced by the large size of the contemporary reindeer population sample, a smaller dataset of modern individuals representing all geographic regions was chosen semi-randomly ( $n=11$ ). The selected samples were T-15, T-7 (Wijdefjorden), B1, B2, T-44 (Central Spitsbergen), C6, C7 (East Svalbard), T-20 (West Spitsbergen), C28 (Nordaustlandet), and B-132, C-84 (South Spitsbergen). Within-population site frequency spectra were calculated with *angsd* v0.931 using the options *-dosaf 1, -gl 1, -noTrans 1, -trim 5, -remove\_bads 1, -minMapQ 30, and -minQ 20*. As described above, the SAF was polarized with ancestral states, and only selected sites and regions were used. The pairwise 2D-SFS was estimated with the *angsd realSFS* tool (Nielsen et al., 2012), and between-population differentiation  $F_{ST}$  values were estimated with *realSFS* commands *fst index* and *fst stats*.

Additionally, an  $F_{ST}$  sliding window analysis was performed as pairwise comparisons among the time groups, using the *angsd realSFS* command *fst stats2* with non-overlapping 10-kbp windows.  $F_{ST}$  values were z-transformed around their mean, and windows with  $z \geq 6$  were defined as outlier windows. The neutrality test statistics Watterson's theta (Watterson, 1975), and Fay and Wu's  $H$  (Fay & Wu, 2000) were calculated within the same windows by using the *angsd realSFS* commands *saf2theta* and *thetaStat do\_stat*. The mean per-site Watterson's theta estimator was used to calculate effective population size ( $N_e$ ) assuming the average mammalian mutation rate of  $2.2 \times 10^{-9}$  per site per year (Kumar & Subramanian, 2002) and a generation time of 6 years as previously estimated for Svalbard reindeer (Flagstad et al., 2022). Mean nucleotide diversity was calculated by dividing pairwise theta by the number of sites in each 10-kbp window.

We further investigated the roles and functions of genes within regions of high divergence between the during-hunting and post-hunting periods, which we defined as regions with mean  $F_{ST} \geq 0.5$ . We retrieved the amino acid sequences of known caribou genes from the annotation provided by Taylor et al. (2019). Amino acid sequences of all 20,014 *Bos taurus* proteins were retrieved from UniProt (UniProt Consortium, 2021) and used to construct a blast protein database with the *makeblastdb* tool within *blast+* v2.6.0 (Altschul et al., 1990). The sequences were identified via a *blastp* search against the *Bos taurus* protein database, only considering results with an *e*-value  $<0.001$ . To select the best matching protein for each query sequence, the result with the smallest *e*-value was chosen. Ties were resolved by first considering highest bit score, then percentage identity, and finally alignment length. We then

identified which protein-coding genes intersect with regions of high divergence.

## 3 | RESULTS

### 3.1 | Read mapping and post-mortem DNA damage assessment

The final dataset consists of 12 Svalbard reindeer with calibrated median age ranging between 3973 and 500 BP (hereafter referred to as the 'pre-hunting' population, Figure 1), six individuals with age ranging between 447 BP and 1950CE (hereafter referred to as the 'during-hunting' population, Figure 1), and 90 present-day individuals (hereafter referred to as the 'post-hunting' population, Figure 1). For genetic comparisons between DNA from subfossil bones/antlers and contemporary samples, the 18 pre-hunting and during-hunting individuals are collectively referred to as the 'ancient' population, and the 90 post-hunting individuals are referred to as the 'modern' population. For the nuclear genome analysis, seven pre-hunting samples were excluded due to their low sequencing depth, resulting in 11 ancient samples.

Nuclear genome raw mapping results are reported in Table S1. After filtering soft-clipped reads and reads with low mapping quality, the mean sequencing depth across all samples (including those that were only used for haplotype network analysis) mapped against the caribou reference assembly was 5.24x (mean ancient DNA: 2.45x; mean modern DNA: 5.80x) (see Table S2). The mean sequencing depth across all samples was slightly higher when mapping against the Svalbard reference genome (mean across all samples: 5.32x; mean ancient DNA: 2.51x; mean modern DNA: 5.88x). The mean sequencing depth of the mitochondrial genome across all samples was 1309.88x (mean ancient DNA: 356.19x; mean modern DNA: 1500.62x). The ancient genomes were confirmed to show characteristic ancient DNA damage patterns (see Figure S5).

### 3.2 | Population structure

In order to assess population structure before, during, and after the period of intense hunting, which resulted in local extirpation followed by recolonization, we performed a PCA of nuclear genome variation and an analysis of genetic admixture based on nuclear genome genotype likelihoods, as well as constructed a haplotype network from mitogenome sequences. To identify patterns in these results, we then analysed them according to the division of Svalbard reindeer metapopulation into 12 spatiotemporal groups.

#### 3.2.1 | Population structure results based on nuclear DNA

After filtering, 42,346 polymorphic nuclear genomic positions were retained for analysis. Except for a few outliers, the post-hunting

genomes cluster based on their geography in the PCA when considering the first two components PC1 and PC2 (**Figure 2**). There was a clear separation of eastern (East Svalbard), northern (Wijdefjorden and Nordaustlandet), and southwestern (Central, South, and West Spitsbergen) individuals. Post-hunting individuals from southern, western, southwestern, and central Spitsbergen form a single tight cluster. The northern groups Nordaustlandet and Wijdefjorden are not as clearly separated from each other, where the Wijdefjorden genomes form a particularly diffuse cluster. The ancient genomes, irrespective of their geographic assignment, form a loose cluster around the centre of the PC2 axis and towards the left of the PC1 axis between the Nordaustlandet, Wijdefjorden, and East Svalbard clusters of post-hunting genomes.

We performed an admixture analysis with a dataset including all individual nuclear genomes (**Figure 3**, **Figures S6** and **S16**). The highest  $\Delta K$  value was found for  $K=4$  (2769.4, **Figure S17**). The assignment of modern groups to estimate genetic clusters strongly correlates with geography, while ancient groups do not. These four major genetic clusters of Svalbard reindeer are a pink cluster, the exclusive component of post-hunting east Svalbard individuals (diversity score [DS]=0) and to a smaller part of south Spitsbergen and Nordaustlandet; a blue cluster, characteristic for west Spitsbergen (DS=0.086) and the major component of Central and South Spitsbergen and a minor component of Wijdefjorden; a green cluster which is the main component of Wijdefjorden (DS=0.242)

and Nordaustlandet (DS=0.693) individuals; and a yellow cluster that is a minor component of central (DS=0.349), west and south Spitsbergen (DS=0.419) and Nordaustlandet. There appears to be a north–south and east–west geographic divide between modern groups, with the northern groups (Wijdefjorden and Nordaustlandet) mainly belonging to the green cluster, southern and western Svalbard mainly belonging to the blue cluster and east Svalbard mainly belonging to the pink cluster. The geographic division becomes more pronounced at higher  $K$  values, where Nordaustlandet develops a private genetic cluster at  $K>5$  (**Figure 3**, **Figures S6** and **S11–S15**) and south Spitsbergen becomes more distinct from west and central Spitsbergen starting at  $K=5$  (**Figure 3**, **Figure S6**) developing a private genetic cluster at  $K>7$  (**Figures S6** and **S13–S15**; **Figure 3**). As expected, there is a high amount of shared ancestry between West Spitsbergen and Central Spitsbergen, the source population from which it was reintroduced (Aanes et al., 2000). Only very little ancestry is shared between East Svalbard and the other groups, and the same is true for Nordaustlandet. Overall, the ancestry assignments agree well with the groupings in the PCA.

In contrast, the spatiotemporal groups of ancient individuals are not strongly distinct from one another in the admixture analysis (**Figure 3**). All groups except during-hunting Wijdefjorden (DS=0) carry ancestry from all four genetic clusters for  $K=4$  (DS 0.440–0.868), irrespective of their geographic distance from one another. Diversity was maintained throughout the hunting period, apart from

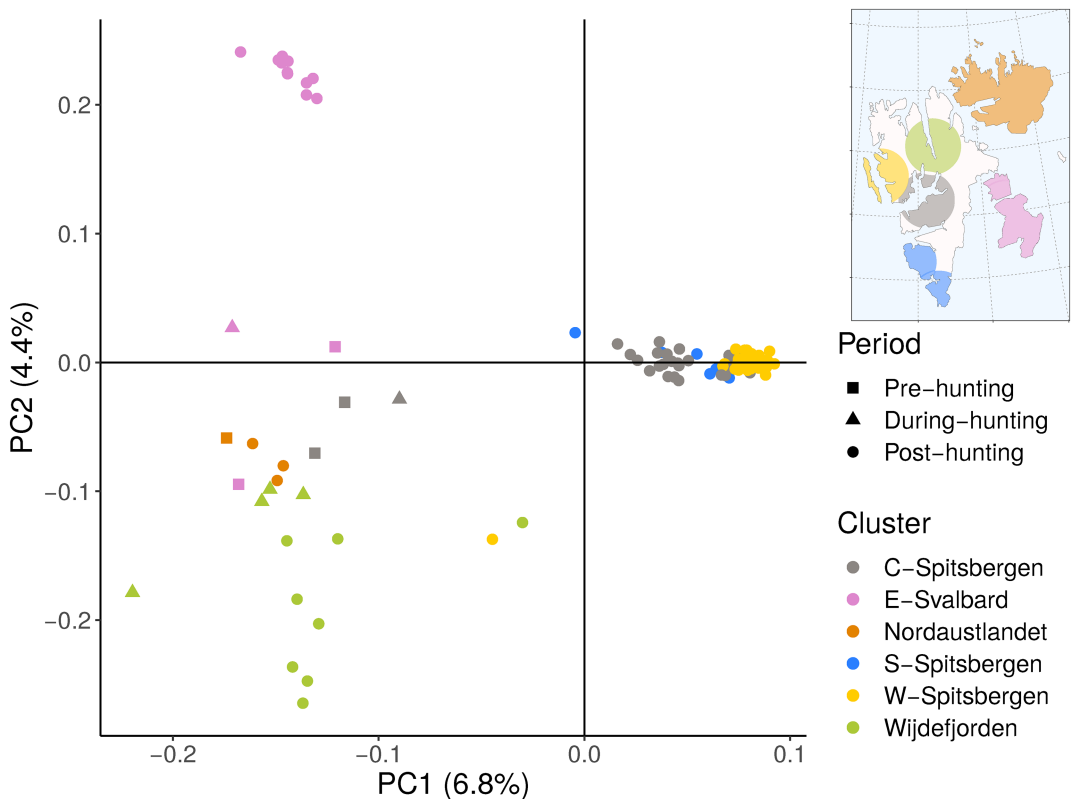


**FIGURE 2** Principal component analysis (PCA) of the genomic variation of Svalbard reindeer. The first two principal components (PCs) are shown. Colour denotes affiliation with a geographic cluster. Shape denotes affiliation with a time period. C-Spitsbergen, Central Spitsbergen; S-Spitsbergen, South Spitsbergen; W-Spitsbergen, West Spitsbergen; E-Svalbard, East Svalbard. [Colour figure can be viewed at [wileyonlinelibrary.com](http://wileyonlinelibrary.com)]

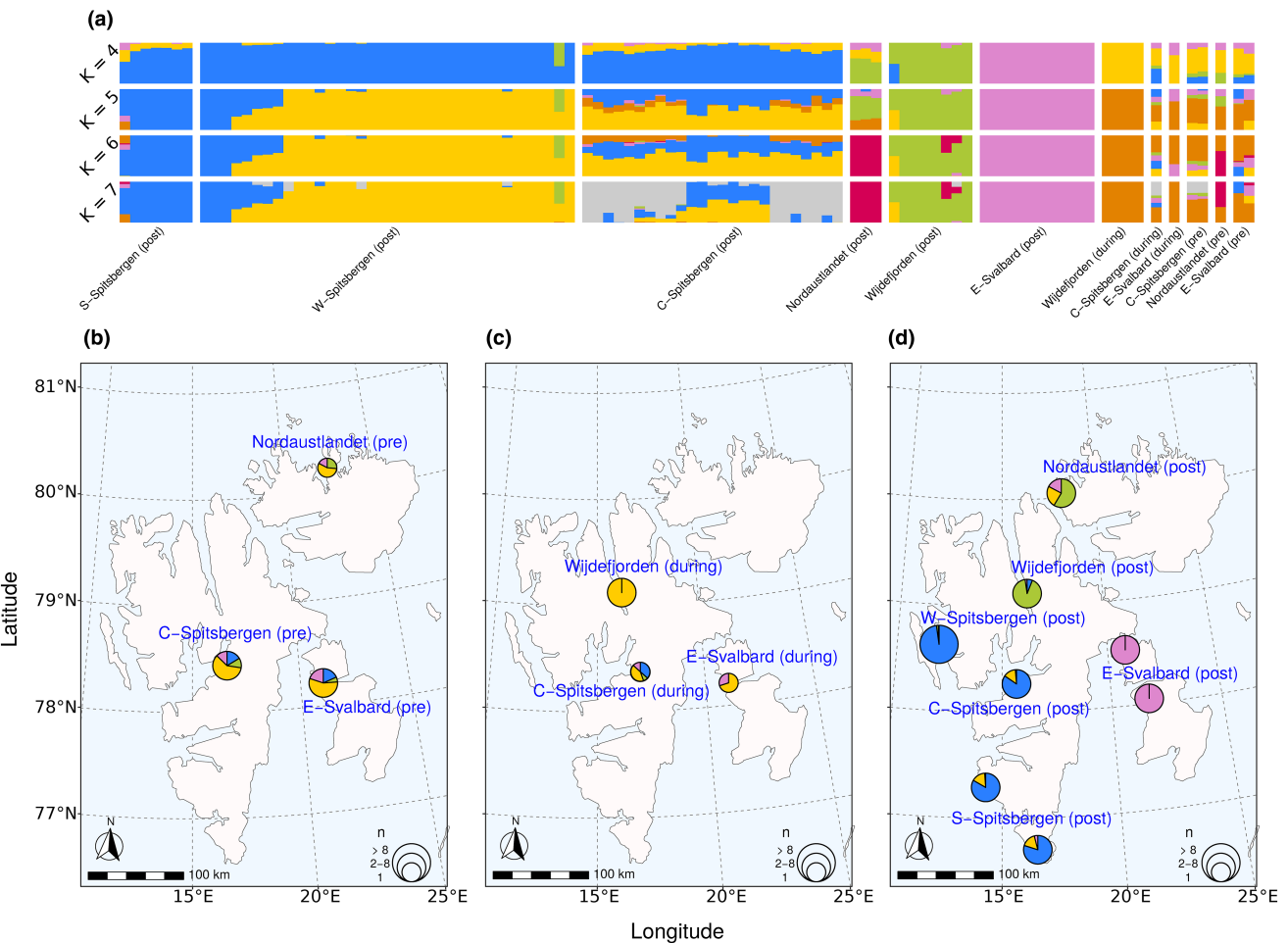


**FIGURE 3** Admixture analysis of Svalbard reindeer in relation to sampling location. (a) Bar plot of admixture proportions for  $K=4$  to  $K=7$ . Each bar represents one individual Svalbard reindeer, and the colour represents affiliation to a proposed ancestral population. Individuals are grouped by spatiotemporal groups as defined by cluster analysis. (b–d) Admixture proportions by sampling location for  $K=4$ . Individuals sampled within 80 km of each other are clustered together into the same pie. Pie size is scaled with the number of individuals. Individual ancestry proportions b before the hunting period, c during the hunting period, and d after the hunting period. C-Spitsbergen, Central Spitsbergen; S-Spitsbergen, South Spitsbergen; W-Spitsbergen, West Spitsbergen; E-Svalbard, East Svalbard. [Colour figure can be viewed at [wileyonlinelibrary.com](http://wileyonlinelibrary.com)]

Wijdefjorden. All ancient individuals share moderate proportions of ancestry with post-hunting Nordaustlandet (yellow) and smaller proportions with post-hunting East Svalbard. This trend continues for values of  $K$  up until  $K=5$ . However, beginning with  $K=6$ , the similarity between post-hunting Nordaustlandet and ancient individuals (except for pre-hunting Nordaustlandet) largely disappears. Instead, we observed the emergence of a new cluster at  $K=5$  (orange) that is shared among all ancient, but only very small proportions of post-hunting individuals are assigned to it. Furthermore, all individuals from during-hunting Wijdefjorden are assigned exclusively to this cluster. As admixture analysis can be biased when having unequal sample sizes (Garcia-Erill & Albrechtsen, 2020; Puechmaille, 2016), we additionally performed an analysis with a reduced sample set with more equal sample sizes by reducing the number of contemporary samples. This analysis confirmed the major results regarding the population structure of the ancient samples that were obtained using the complete dataset (Figure S16). For example, at  $K=4$ , all ancient samples share high proportions of private ancestry (green),

except for pre-hunting Nordaustlandet, which shows high affinity to modern Nordaustlandet and Wijdefjorden (Figure S16).

### 3.2.2 | Population structure results based on mitochondrial DNA

We found 30 distinct haplotypes (32 including the outgroup samples from Franz Joseph Land) from the mitogenome alignment of 108 individuals, and none of these haplotypes were shared between individuals in the pre- and post-hunting period (Figure 4). However, haplotype relatedness does not group per time period. Instead, post-hunting haplotypes were primarily at the periphery of the network, branching from different ancient ancestors located at the centre of the network (Figure 4). Half of these 30 haplotypes belonged to 18 individuals from the ancient populations, while the other half belonged to the 90 individuals from the post-hunting populations. The outgroup samples from Franz Joseph Land root

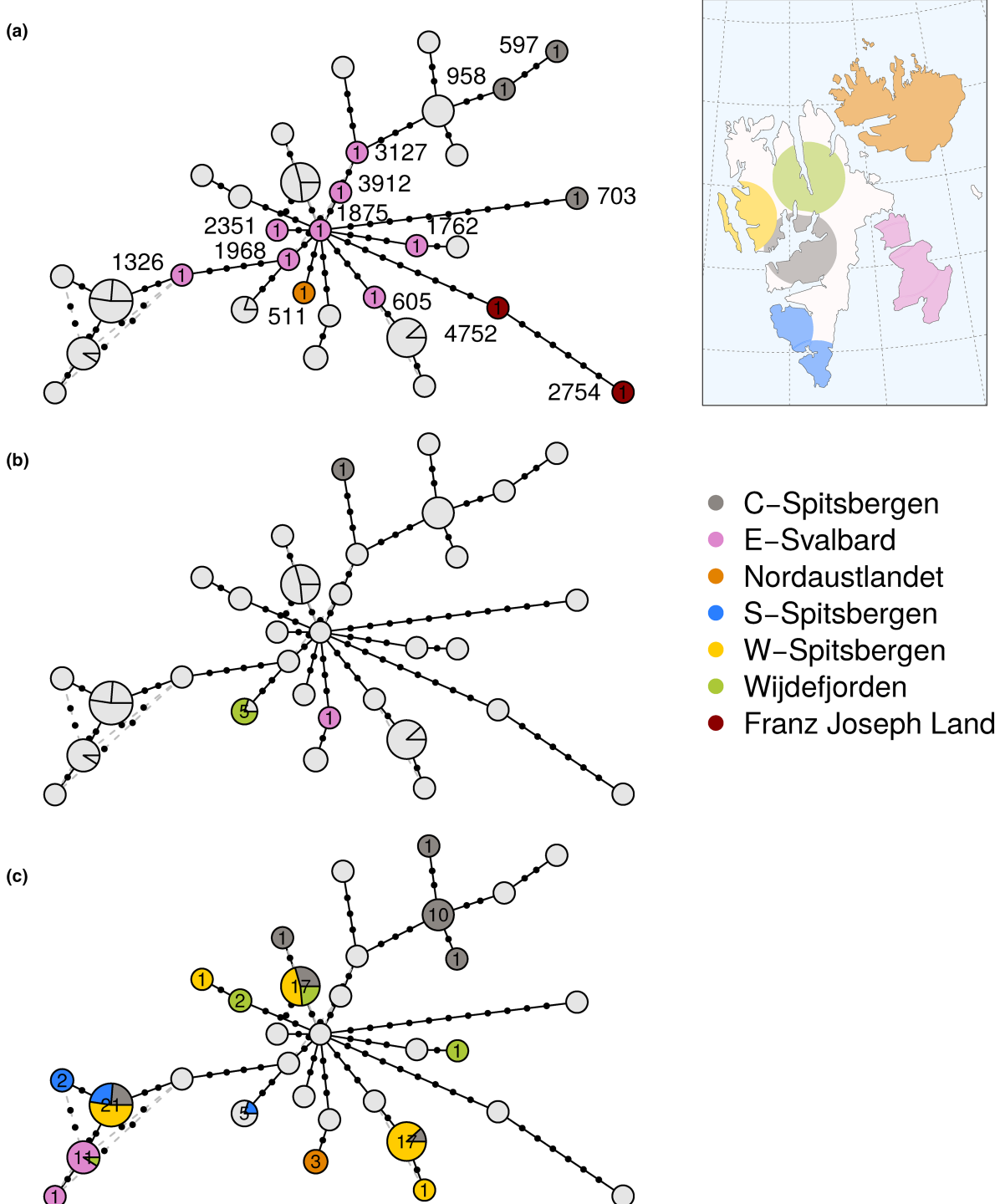


**FIGURE 4** Haplotype network of Svalbard reindeer mitogenomes during three temporal hunting periods. (a) Pre-hunting. (b) During-hunting. (c) Post-hunting. The network includes two mitogenomes from the extinct population of reindeer from the arctic archipelago of Franz Josef Land (not shown on map) as outgroups. The number of individuals sharing the same haplotype is indicated in the centre of the circle. Light grey circles indicate the positioning of haplotypes that do not belong to the time period in focus. The diameter of the circles indicates the number of individuals sharing that haplotype and is scaled from 1 (i.e., min. haplotype number of 1) to 2 (i.e., max. haplotype number of 21). In the pre-hunting period, calibrated carbon-dated ages are reported as the median age probability in years before present (before 1950 AD). Calibrated age ranges are reported in Table 1. C-Spitsbergen, Central Spitsbergen; S-Spitsbergen, South Spitsbergen; W-Spitsbergen, West Spitsbergen; E-Svalbard, East Svalbard. [Colour figure can be viewed at [wileyonlinelibrary.com](http://wileyonlinelibrary.com)]

at the oldest Svalbard samples (East Svalbard) at the centre of the network. Each of the 12 individuals from the pre-hunting period had distinct haplotypes with up to 32 segregating sites. Individuals

from the same region (i.e., East Svalbard) had only 1–3 segregating sites despite the thousands of years separating the sampled individuals (e.g., East Svalbard, 2037 years difference for only one

segregation site difference). However, some individuals from the same region, living at approximately the same time (e.g., Central Spitsbergen, 597 and 703 BP), have the most divergent haplotypes for the given region and are even more distant than Franz Joseph Land outgroups. In the during-hunting period, four out of six individuals (66%) shared the same haplotype, and those were from the same region, Wijdefjorden. In the post-hunting period, we found up to 36 different segregation sites, forming seven distinct haplogroups separated by fewer than three mutations, where several individuals from the same region shared the same haplotype. However, within the same region, we also found very distant haplotypes with individuals more closely related to their common ancestral haplotype than to one another. For instance, in the Central Spitsbergen region, modern haplotypes were either closely related to the haplotypes previously found in that same region or previously found in Eastern-Svalbard. Therefore, haplotypes found today within the same region are more distant than haplotypes currently found across regions. Subsequently, although mitochondrial haplotype and nucleotide diversity were lower in the post-hunting than in the pre-hunting period, they have not been drastically reduced by hunting (Table 2).

### 3.3 | Temporal genomic differentiation

Heterozygosity decreased stepwise through the hunting periods, from the highest in the pre-hunting group to the lowest in the post-hunting group, although there was considerable overlap between the heterozygosity ranges of the three groups (see Figure 5). The median heterozygosities are  $3.8 \times 10^{-4}$  for the pre-hunting period,  $3.1 \times 10^{-4}$  for the during-hunting period, and  $2.8 \times 10^{-4}$  for the post-hunting period (Table 2). The differences in mean heterozygosity between during-hunting and the other two groups are not significant (pre-hunting:  $p=.66$ , post-hunting:  $p=.10$ , Mann–Whitney  $U$  test), while post-hunting heterozygosity is significantly lower than pre-hunting ( $p<.01$ , Mann–Whitney  $U$  test). Note that despite the small sample size in the pre-hunting group ( $n=5$ ), the power to correctly

reject that the pre-hunting group did not have a higher mean than the post-hunting group was high ( $1-\beta=0.96$ , one-sided two-sample  $t$ -test). The decrease in median heterozygosity from pre-hunting to during-hunting reindeer is 18%, and post-hunting reindeer have a 10% lower median heterozygosity than during-hunting reindeer. The median heterozygosity of post-hunting reindeer is 26% lower than that of pre-hunting reindeer. Effective population size in the pre-hunting period was  $5.21 \times 10^3$ . It increased by 10% to  $5.84 \times 10^3$  by the time of the during-hunting period. It subsequently dropped by 20% to  $4.66 \times 10^3$  in the post-hunting period. In the sliding window analysis, the mean nucleotide diversity across all windows was  $3.34 \times 10^{-4}$  in the pre-hunting population, slightly higher at  $3.35 \times 10^{-4}$  in the during-hunting population and reduced to  $3.23 \times 10^{-4}$  in the post-hunting population.

There were a total of 217,247 windows identified by the sliding window analysis, of which 183 (0.1%) were  $F_{ST}$  outlier windows as defined by a  $Z$ -score  $\geq 6$  (Figure 6). The mean value of weighted pairwise  $F_{ST}$  was  $1.91 \times 10^{-2}$  for the pre-hunting and during-hunting populations,  $3.27 \times 10^{-2}$  for the pre-hunting and post-hunting populations, and  $5.06 \times 10^{-2}$  for the during-hunting and post-hunting populations. The mean number of sites across all windows was 8649, and the mean number of sites within outlier windows was 8843. To assess whether windows were under positive selection, we performed neutrality tests to compare Fay & Wu's  $H$  between during-hunting outlier and non-outlier windows, as well as between post-hunting outlier and non-outlier windows. Comparison shows that  $H$  is much lower and more broadly distributed in ancient outlier windows compared to all the other groups (Figure 6 and Figure S18).

To explore any functional genetic changes that may have resulted from overhunting and near-extirpation of Svalbard reindeer, we further investigated those outlier genomic regions with extraordinarily high  $F_{ST}$  ( $F_{ST} \geq 0.5$ ) as measured between the during-hunting and post-hunting populations, as well as the identity and functions of the genes therein (Table S4). We identified 50 high-divergence outlier windows which intersect with genes, of which

TABLE 2 Measures of diversity statistics from the mitogenome analysis and genomic diversity.

Time period	Mitochondrial genome					Nuclear genome				
	N	Num. Haplo.	Num. Seg. Sites	Hap. div.	Nuc. div.	N	Mean ( $\pm$ SD). Med. het.		Nuc. div.	$N_e$
							Mean ( $\pm$ SD)	Med. het.		
Pre-hunting	12	12	32	$1.00 \pm 5.79E-04$	$4.88E-04$	5	$3.8E-04$	$(\pm 7.3E-05)$	$3.8E-04$	$3.34E-04$
During-hunting	6	3	13	$0.60 \pm 4.54E-02$	$3.03E-04$	6	$3.9E-04$	$(\pm 1.5E-04)$	$3.1E-04$	$3.35E-04$
Ancient (Pre- and During-hunting)	18	15	40	$0.96 \pm 11.01E-04$	$4.84E-04$	11	$3.9E-04$	$(\pm 1.2E-04)$	$3.4E-04$	
Post-hunting	90	15	36	$0.85 \pm 2.42E-04$	$4.50E-04$	89	$2.9E-04$	$(\pm 4.4E-05)$	$2.8E-04$	$3.23E-04$
All genomes	108	30	56	$0.90 \pm 1.80E-04$	$5.16E-04$	100	$3.0E-04$	$(\pm 6.4E-05)$	$2.9E-04$	$4.66E+03$

Abbreviations: Hap. div, haplotype diversity and its standard deviation; Med. het., median heterozygosity; N, number of individuals;  $N_e$ , effective population size; Nuc. div, nuclear diversity; Nuc. div., nucleotide diversity; Num. haplo., Number of haplotypes; Num. seg. sites., Number of segregation sites.

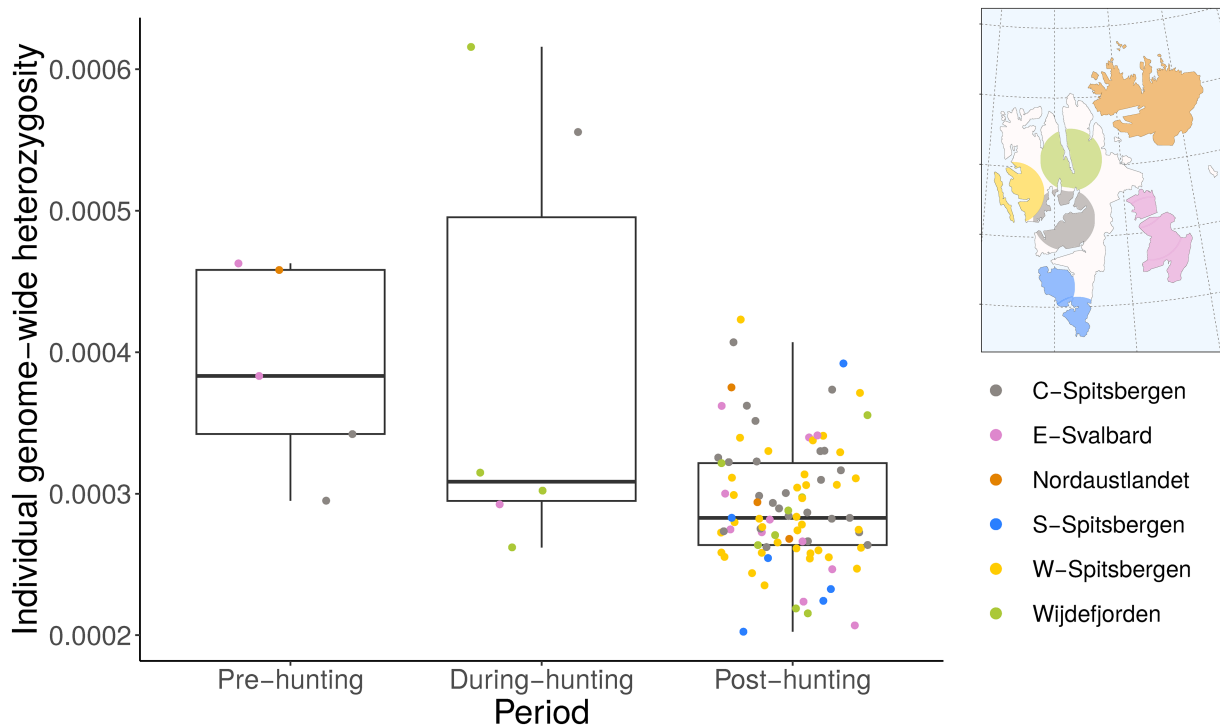


**FIGURE 5** Individual genome-wide heterozygosity by time period. The points are horizontally scattered to increase visibility. Thick horizontal line in the boxplot represents the median, the lower and upper box bounds represent the 25 and 75 percentiles, respectively. C-Spitsbergen, Central Spitsbergen; S-Spitsbergen, South Spitsbergen; W-Spitsbergen, West Spitsbergen; E-Svalbard, East Svalbard. [Colour figure can be viewed at [wileyonlinelibrary.com](https://wileyonlinelibrary.com)]

34 are unique annotated genes (Taylor et al., 2019). A blastp search against the *Bos taurus* proteome (see Materials and Methods) matched 30 of these 34 genes to 29 unique *Bos taurus* proteins (Table S4). Of these 29, 17 are predicted proteins, 9 are further inferred from homology, and 4 have evidence at transcriptome level. For 17 of these proteins, the associated coding gene is known in the UniProt database. The known coding genes are PLCH1, TRIM72 (MG53), TIMM17B, ANP32B, APBA1, BLNK, CCNA1, DAB2IP, EBF2/COE2, HS3ST2, LOC529488, NRXN1, RABGAP1, SF3B1, SFMBT1, STRBP, and TTC39B.

## 4 | DISCUSSION

Here, by combining modern and the first ancient genomes (up to 4000 BP), we have described and compared the population structure and genetic changes of Svalbard reindeer before, during, and after an intense period of anthropogenic harvest. We have shown that the population collapse due to overharvest decreased nuclear genomic diversity as well as effective population size (Figure 5, Table 2). The overhunting event also resulted in a shift of genetic diversity across the entire archipelago (Figures 2 and 3), suggesting weaker population substructure before human presence and harvest. Mitogenome analysis also revealed a significant loss, with none of the pre-hunting haplotypes occurring today (Figure 4, Table 2). Hence, post-hunting haplotypes formed their own haplogroups, which were more closely linked to ancient haplotypes from different

regions of Svalbard than to the ancient haplotypes from their respective sampling locations. Gene selection analyses indicate pronounced genetic drift during and post-hunting periods rather than natural selection (Figure 6).

### 4.1 | Major changes in population structure and differentiation

Our analysis of population structure based on whole nuclear genomes revealed substantial differences between ancient and present-day Svalbard reindeer (Burnett et al., 2023; Peeters et al., 2020). Specifically, the ancient population possesses unique ancestry that is largely unidentified in the modern population. Although we identified  $K=4$  as the optimal value of  $K$  with the delta- $K$  method, in light of potential sampling bias and strong population structure in both space and time, we see the importance of discussing higher values of  $K$  as well. In contrast to the high degree of genetic differentiation in the post-hunting populations, which show a near-perfect correspondence of geographical and genetic grouping, Svalbard reindeer did not form distinct genetic clusters based on location prior to and during hunting. Instead, all geographic areas but one (Wijdefjorden) had higher nuclear genetic diversity in the pre-hunting period. Pre-hunting Svalbard reindeer individuals also showed affinity to all post-hunting metapopulations for  $K=2$  to  $K=7$ , which suggests a scenario where Svalbard reindeer experienced higher levels of gene flow between different geographic regions in the past. A similar situation has been reported for

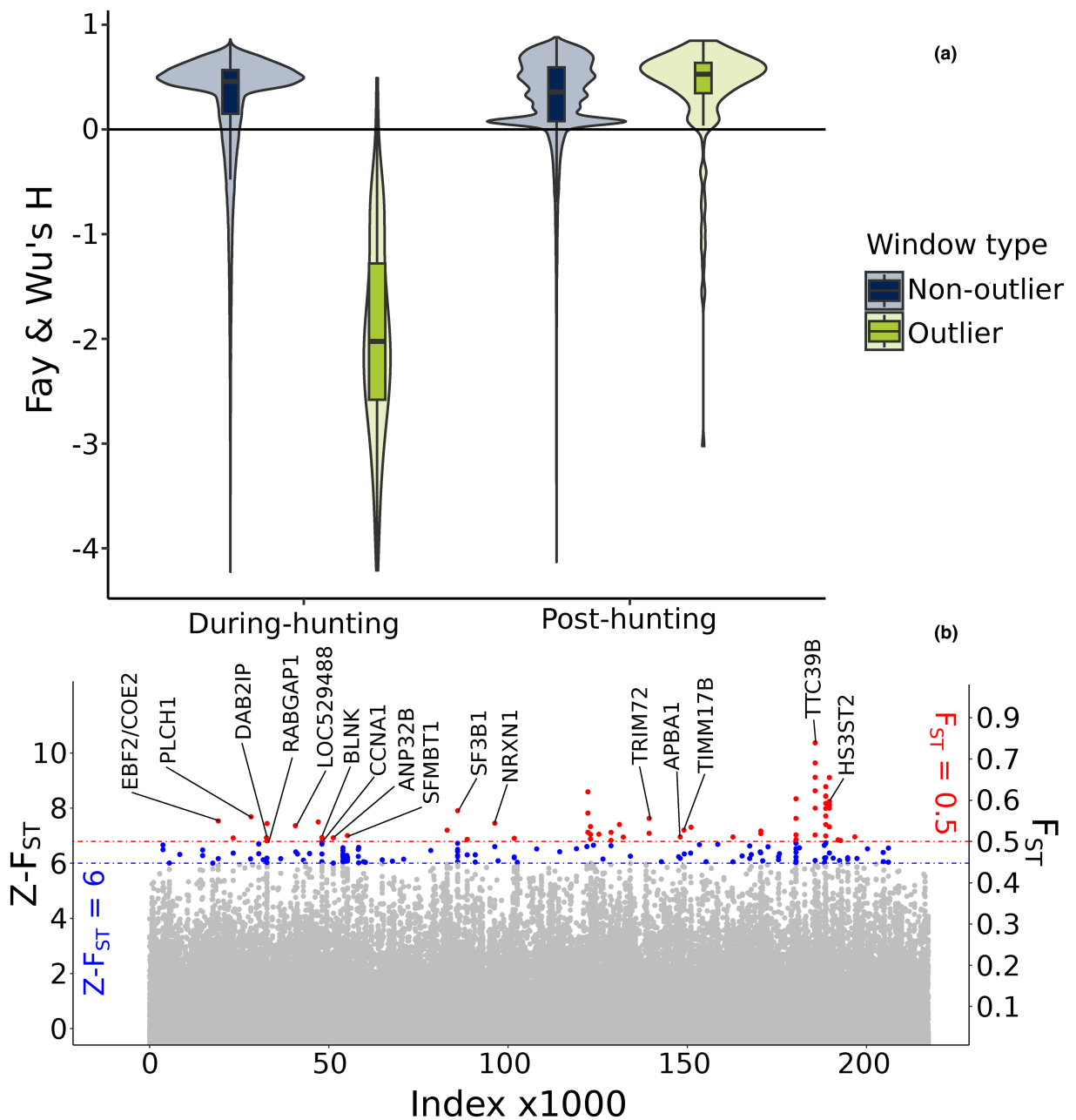


**FIGURE 6** Outlier genomic windows and their genes. (a) Comparison of Fay & Wu's  $H$  in genomic windows as measure of neutrality. Here,  $H$  was measured in genomic regions (windows) in genomes of individuals living during- (left) and post-hunting (right). Regions that strongly diverged ( $ZFST \geq 6$ ) between the during-hunting and post-hunting time periods are called 'outliers' (green), those that are not 'non-outliers' (blue). Each violin shows the distribution of  $H$  in each type/period pair, respectively. (b) Manhattan plot of genomic windows, highlighting windows that cross the threshold of  $ZFST$  greater than or equal to 6 (blue) and  $FST$  of greater than or equal to 0.5 (red). High  $FST$  windows that intersect with described genes are labelled with the gene name. [Colour figure can be viewed at [wileyonlinelibrary.com](http://wileyonlinelibrary.com)]

the Iberian lynx (*Lynx pardinus* (Temminck, 1827)), another species with a severe history of overharvest (Casas-Marce et al., 2017). Changes in population structure happened between the during-hunting and post-hunting groups, rather than between the pre-hunting and during-hunting groups, which cover a much longer time span, suggesting that the change was a consequence of overharvest. Nevertheless, given our limited sample size of ancient nuclear genomes spanning a long time frame, it may not be possible to fully characterize the spatial distribution of genetic structure of ancient Svalbard reindeer. Further

efforts to sequence additional genomes from ancient Svalbard will be useful for further resolving the degree of genetic structure and gene flow that existed prior to human disturbance.

Individuals from modern Nordaustlandet were most similar to their ancient counterparts for all values of  $K$ . The reasons for this are likely the absence of harvest-induced bottleneck due to the remoteness of this location, inaccessible for most of the year due to sea-ice cover and the small size of this remnant population which remained low, surviving in a sparsely vegetated polar desert (Le

Moullec et al., 2019). On the contrary, other remnant populations underwent rapid population growth and geographic expansion (Le Moullec et al., 2019). This interpretation is supported by the PCA, which places modern Nordaustlandet closer to the ancient samples than any other modern population. This indicates there is potential value in conservation of the Nordaustlandet population, which has perhaps not experienced population crashes and genetic drift to the same extent as the populations on other islands.

We observed a gradual decrease in Svalbard reindeer genome heterozygosity over the three time periods. Median heterozygosity was reduced by 26% over the time spanning the pre-hunting and the post-hunting periods. This decrease is congruent with results obtained from previous studies comparing modern to historic/ancient vertebrates that underwent large-scale population declines due to anthropogenic near-extirpation events, for example, the white rhinoceros (*Ceratotherium simum* (Burchell, 1817), Sánchez-Barreiro et al., 2021), alpine ibex (*Capra ibex*, Linnaeus, 1758, Robin et al., 2022), eastern gorilla (*Gorilla beringei*, Matschie, 1903, van der Valk et al., 2019), and iberian lynx (Casas-Marce et al., 2017). The Svalbard reindeer's decrease of heterozygosity over time is of similar severity to that measured following drastic population declines in the Iberian lynx (heterozygosity reduction of 10% based on microsatellite data (Casas-Marce et al., 2017)) and in two over-harvested populations of white rhinoceros (heterozygosity reductions of 10% and 37% respectively, Sánchez-Barreiro et al., 2021). A study by van der Valk et al. (2019) reported a 20% decrease of heterozygosity in Grauer's gorillas but only a 3% decrease in mountain gorillas. It is important to note that prior to overharvesting, genome-wide heterozygosity in the Svalbard reindeer population was already among the lowest levels observed in mammals (Pečnerová et al., 2023, and Figure 5 therein), perhaps because of the strong bottleneck they experienced during the colonization of Svalbard (Dussex et al., 2023).

Our analysis of temporal change in mitogenome diversity did not reveal any evidence of a major decrease in genetic diversity. The relatively high diversity of modern haplogroups ( $n=7$ ) contrasts with other ungulate species heavily hunted in the past, like the Alpine ibex, where only two modern haplogroups are now widespread across their range (Robin et al., 2022). Contrary to the Alpine ibex, in which mitogenome nucleotide diversity was reduced by  $\sim 79\%$  ( $6.38 \times 10^{-4}$ ) from the pre-hunting to the post-hunting period, Svalbard reindeer experienced a reduction of only  $\sim 8\%$  ( $0.38 \times 10^{-4}$ ). However, this difference could be explained by the fact that after near-extirpation, the Svalbard reindeer survived in four remnant populations, as opposed to the Alpine ibex, which survived in only a single remnant population. During the intermediate hunting period, the mitogenome nucleotide diversity surprisingly dropped, yet this is likely due to the low sample size. In this period, large individual variation existed, where two of the six individuals had the highest genome-wide heterozygosity observed in our dataset, while the other four were among the lowest values. The uncertainty related to the carbon-dating calibration scale prior to the industrial era, which coincides with our during-intermediate hunting period (1500–1950CE), restricts the temporal resolution of this period.

However, previous reports documented a harvest peak in the early 1900s CE (Hoel, 1916; Lønø, 1959), just prior to the legal protection of Svalbard reindeer in 1925. Thus, individuals with high genetic diversity are likely to have lived prior to this harvesting peak.

## 4.2 | Potential climate change impacts during recovery

Accounting for the fact that current summer temperature has already increased by 1.5–2°C since the reference period of 1912–2012CE (Isaksen et al., 2022; van der Bilt et al., 2019), the older reindeer specimens from our collection (ages of 3000–4000 BP) experienced summer temperatures that were similar to the present-day climate. From this period and until harvesting started  $\sim 1500$  CE, the relatively stable climate became gradually cooler with sea-ice cover persisting year-round (Werner et al., 2016), likely acting as dispersal corridors for reindeer. These conditions likely favoured a higher degree of admixture between populations.

The current population structuring is a consequence of overharvesting and recovery occurring during a period of pronounced climate warming. Our results are congruent with earlier findings based on microsatellite data and nuclear whole-genome sequencing where present-day population structuring reflects the recolonization patterns originating from the four locations that escaped extirpation (Burnett et al., 2023; Peeters et al., 2020). In addition to the sedentary behaviour of the Svalbard reindeer, the effect of natural barriers for dispersal and gene flow has increased during the recovery period, as sea-ice cover decreased (Peeters et al., 2020). Despite this, Svalbard reindeer were capable to disperse naturally and through reintroduction events to all suitable habitats on Svalbard within a century after protection (Le Moullec et al., 2019). The increased isolation due to sea-ice cover decline may have been partly counteracted by recent increases in frequency of rain-on-snow events resulting in winters with poor feeding conditions (Peeters et al., 2019). That is, such extreme events can sometimes aid recolonization by 'pushing' reindeer to disperse to neighbouring islands or peninsulas where they were previously extirpated (Hansen et al., 2011). This may have accelerated the natural recolonization process, likely through a stepping-stone process that conserves geographic genetic structuring, but also likely further decreased genetic diversity in the peripheral recolonized populations. Still, the rapid increase in temperatures in Svalbard (Isaksen et al., 2022) and associated sea-ice decline likely restrict dispersal more nowadays than over the millennia prior to anthropogenic disturbance.

## 4.3 | Stochastic changes within diverse gene families

For the pre-hunting and during-hunting populations, we observed strongly negative values of Fay & Wu's  $H$  within  $F_{ST}$  outlier windows,

whereas these  $F_{ST}$  outlier windows had generally positive  $H$  values in the post-hunting population. This indicates that these genomic regions were experiencing positive selection in the pre-hunting and during-hunting periods, but now evolve mainly under genetic drift in the extant post-hunting population, rather than by natural selection (Fay & Wu, 2000). Conceivably, selection pressures from the extreme Arctic environment were the major force acting on Svalbard reindeer under natural conditions prior to anthropogenic disturbance. However, genetic drift can rapidly and stochastically alter allele frequencies, including at loci that were previously conserved under strong selective pressures, especially in small populations (Bortoluzzi et al., 2020). Future research would be needed to confirm whether there are functional consequences, for example, affecting fecundity, survival, or behaviour.

In that context, it is relevant to explore which genes were most affected by genetic drift following overhunting, since they may have functional relevance for the health and conservation of the present-day Svalbard reindeer population. Owing to the stochastic nature of genetic drift, the affected genes and their coded proteins are involved in a variety of biological functions (see also Appendix S1). However, among the candidate genes we identified are some that play key roles in circadian rhythm regulation and fat storage. The loss of a day/night controlled internal biological clock is considered an important adaptation of reindeer to high-arctic environments, where daylight conditions do not change for extended periods of the year (Lin et al., 2019; van Oort et al., 2005). In addition, the Svalbard reindeer's overwinter survival is dependent on its ability to build up high ratios of body fat relative to total body mass over the very short snow-free season (Trondrød et al., 2021), normally lasting for about 3–4 months. It is not unlikely that the genes linked to excessive fat accumulation (i.e., obesity) in other species are the same underlying genes that support rapid fattening in Svalbard reindeer. Thus, the observed changes in allele frequency of these genes involved in key adaptive traits to the high-arctic environment may impact the fitness of Svalbard reindeer.

#### 4.4 | Implications for conservation

Our study supplements a growing body of research utilizing temporal datasets to assess genomic health of threatened and endemic species. Our analyses indicate that historical overharvest has, in addition to the previously reported population size reduction (Lønø, 1959), decreased overall genomic diversity in Svalbard reindeer. While subsequent protection of the Svalbard reindeer and its habitat has rapidly (i.e., rapidly in an evolutionary context) facilitated the recolonization of the archipelago (Le Moullec et al., 2019), the current level of genome erosion could make this subspecies particularly vulnerable to future climate and environmental changes and associated demographic stochasticity, especially if inbreeding levels remain high (Burnett et al., 2023; Peeters et al., 2020). Our findings support the view that census data on population abundances alone

is not robust enough to assess the conservation status of populations recovering from overharvest or other anthropogenic stressors. Genomic monitoring, especially when incorporating a temporal component derived from ancient DNA, can help capture a more complete understanding (Jensen et al., 2022).

In combination with such genomic monitoring, translocations have been suggested as an effective conservation measure (Bertola et al., 2022; Bubac et al., 2019). In contrast to other species (e.g., Iberian and Alpine ibex; Grossen et al., 2018, 2020), translocation events have strongly contributed to limit the genetic diversity loss in Svalbard reindeer caused by overharvesting, likely because the translocated individuals came from the population with the highest genetic diversity levels (Burnett et al., 2023). Nevertheless, a population's adaptive potential relies not only on their overall level of genetic diversity but also on functional diversity. When the genetic diversity of a species is low and there has been significant genetic turnover due to genetic drift rather than natural selection—as in Svalbard reindeer—the species' capacity to evolve with climate change has possibly been reduced.

#### AUTHOR CONTRIBUTIONS

FLK, MLM wrote the paper with input from all authors. FLK, MLM analysed data with input from MDM, VCB, JCB, HB. FLK, MLM, MDM, VCB, ND, BP contributed to interpreting the results. MRE, VCB, MDM, BP did ancient DNA lab work. MLM, BBH, JR performed ancient sample acquisition and preparation. BBH, MLM, MDM had the original idea for the study. FLK, MLM, MDM, BBH, JR, BP, VCB designed the study. MDM, VCB supervised the palaeogenomic work. MDM, BBH funded the study.

#### ACKNOWLEDGEMENTS

We thank M. Thomas P. Gilbert for his valuable financial support of the computational analyses. We are grateful to Marie-Josée Nadeau and Martin Seiler at the National Laboratory of Age Determination, NTNU and to Love Dalén for support and advice early in the project period. We acknowledge the following sequencing centres and associates for their invaluable services: Novogene (Cambridge, UK), the Norwegian National Sequencing Centre (Oslo, Norway), and the NTNU Genomics Core Facility (Trondheim, Norway). Some computational analyses were performed on resources provided by the Danish National Life Science Supercomputing Center (Computerome) and the National Infrastructure for High-Performance Computing and Data Storage in Norway (UNINETT Sigma2) under projects NN8052K and NS8052K. We thank the field assistants, the Norwegian Polar Institute and University Centre in Svalbard for logistical assistance, as well as Børge Ousland for providing the samples from his expedition to Franz Joseph Land, on the return from the North Pole in 2007.

#### CONFLICT OF INTEREST STATEMENT

The authors declare no conflicts of interest.

## DATA AVAILABILITY STATEMENT

Raw sequence data generated for this study has been archived at the European Nucleotide Archive under accession code PRJEB60484. Sample metadata can be accessed in the supplementary material (Table S3). The alignment of mitogenome sequences analysed in this study is available on the data repository Dryad (DOI: [10.5061/dryad.tht76hf5n](https://doi.org/10.5061/dryad.tht76hf5n)).

## ORCID

- Fabian L. Kellner  <https://orcid.org/0000-0002-9057-3018>  
 Mathilde Le Moullec  <https://orcid.org/0000-0002-3290-7091>  
 Martin R. Ellegaard  <https://orcid.org/0000-0001-5777-091X>  
 Jørgen Rosvold  <https://orcid.org/0000-0001-9555-5217>  
 Bart Peeters  <https://orcid.org/0000-0002-2341-1035>  
 Hamish A. Burnett  <https://orcid.org/0000-0002-1868-4944>  
 Åshild Ørnvik Pedersen  <https://orcid.org/0000-0001-9388-7402>  
 Jaelle C. Brealey  <https://orcid.org/0000-0001-7068-2017>  
 Nicolas Dussex  <https://orcid.org/0000-0002-9179-8593>  
 Vanessa C. Bieker  <https://orcid.org/0000-0002-2061-9041>  
 Brage B. Hansen  <https://orcid.org/0000-0001-8763-4361>  
 Michael D. Martin  <https://orcid.org/0000-0002-2010-5139>

## REFERENCES

- Aanes, R., Saether, B.-E., & Ørntsland, N. A. (2000). Fluctuations of an introduced population of Svalbard reindeer: The effects of density dependence and climatic variation. *Ecography*, 23(4), 437–443.
- Albon, S. D., Irvine, R. J., Halvorsen, O., Langvatn, R., Loe, L. E., Ropstad, E., Veiberg, V., van der Wal, R., Bjørkvol, E. M., Duff, E. I., Hansen, B. B., Lee, A. M., Tveraa, T., & Stien, A. (2017). Contrasting effects of summer and winter warming on body mass explain population dynamics in a food-limited Arctic herbivore. *Global Change Biology*, 23(4), 1374–1389.
- Allendorf, F. W., & Hard, J. J. (2009). Human-induced evolution caused by unnatural selection through harvest of wild animals. *Proceedings of the National Academy of Sciences of the United States of America*, 106(Suppl 1), 9987–9994.
- Altschul, S. F., Gish, W., Miller, W., Myers, E. W., & Lipman, D. J. (1990). Basic local alignment search tool. *Journal of Molecular Biology*, 215(3), 403–410.
- Bana, N. Á., Nyiri, A., Nagy, J., Frank, K., Nagy, T., Stéger, V., Schiller, M., Lakatos, P., Sugár, L., Horn, P., Barta, E., & Orosz, L. (2018). The red deer *Cervus elaphus* genome CerEla1.0: Sequencing, annotating, genes, and chromosomes. *Molecular Genetics and Genomics*, 293(3), 665–684.
- Bertola, L. D., Miller, S. M., Williams, V. L., Naude, V. N., Coals, P., Dures, S. G., Henschel, P., Chege, M., Sogbohossou, E. A., Ndiaye, A., Kiki, M., Gaylard, A., Ikanda, D. K., Becker, M. S., & Lindsey, P. (2022). Genetic guidelines for translocations: Maintaining intraspecific diversity in the lion (*Panthera leo*). *Evolutionary Applications*, 15(1), 22–39.
- Bortoluzzi, C., Bosse, M., Derkx, M. F. L., Crooijmans, R. P. M. A., Groenen, M. A. M., & Megens, H.-J. (2020). The type of bottleneck matters: Insights into the deleterious variation landscape of small managed populations. *Evolutionary Applications*, 13(2), 330–341.
- Bowyer, R. T., Boyce, M. S., & Goheen, J. R. (2019). Conservation of the world's mammals: Status, protected areas, community efforts, and hunting. *Journal of Mammalogy*, 100, 923–941.
- Bubac, C. M., Johnson, A. C., Fox, J. A., & Cullingham, C. I. (2019). Conservation translocations and post-release monitoring: Identifying trends in failures, biases, and challenges from around the world. *Biological Conservation*, 238, 108239.
- Burnett, H. A., Bieker, V. C., Le Moullec, M., Peeters, B., Rosvold, J., Pedersen, Å. Ø., Dalén, L., Loe, L. E., Jensen, H., Hansen, B. B., & Martin, M. D. (2023). Contrasting genomic consequences of anthropogenic reintroduction and natural recolonization in high-arctic wild reindeer. *Evolutionary Applications*, 16(9), 1531–1548.
- Byun, S. A., Koop, B. F., & Reimchen, T. E. (2002). Evolution of the Dawson caribou (*Rangifer tarandus dawsoni*). *Canadian Journal of Zoology*, 80(5), 956–960.
- CAFF. (2013). Arctic biodiversity assessment: Status and trends in Arctic biodiversity. *Conservation of Arctic Flora and Fauna* (H. Meltofte (ed.)). CAFF International Secretariat.
- Carøe, C., Gopalakrishnan, S., Vinner, L., Mak, S. S. T., Sinding, M. H. S., Samaniego, J. A., Wales, N., Sicheritz-Pontén, T., & Gilbert, M. T. P. (2018). Single-tube library preparation for degraded DNA. *Methods in Ecology and Evolution / British Ecological Society*, 9(2), 410–419.
- Casas-Marce, M., Marmesat, E., Soriano, L., Martínez-Cruz, B., Lucena-Perez, M., Nocete, F., Rodríguez-Hidalgo, A., Canals, A., Nadal, J., Detry, C., Bernáldez-Sánchez, E., Fernández-Rodríguez, C., Pérez-Ripoll, M., Stiller, M., Hofreiter, M., Rodríguez, A., Revilla, E., Delibes, M., & Godoy, J. A. (2017). Spatiotemporal dynamics of genetic variation in the Iberian lynx along its path to extinction reconstructed with ancient DNA. *Molecular Biology and Evolution*, 34(11), 2893–2907.
- Chang, C. C., Chow, C. C., Tellier, L. C., Vattikuti, S., Purcell, S. M., & Lee, J. J. (2015). Second-generation PLINK: Rising to the challenge of larger and richer datasets. *GigaScience*, 4, 7.
- Collard, R.-C., Dempsey, J., & Holmberg, M. (2020). Extirpation despite regulation? Environmental assessment and caribou. *Conservation Science and Practice*, 2(4), e166. <https://doi.org/10.1111/csp.12166>
- Crema, E. R., & Bevan, A. (2021). Inference from large sets of radiocarbon dates: Software and methods. *Radiocarbon*, 63(1), 23–39.
- Derocher, A. E., Wiig, Ø., & Bangjord, G. (2000). Predation of Svalbard reindeer by polar bears. *Polar Biology*, 23(10), 675–678.
- Díez-Del-Molino, D., Sánchez-Barreiro, F., Barnes, I., Gilbert, M. T. P., & Dalén, L. (2018). Quantifying temporal genomic erosion in endangered species. *Trends in Ecology & Evolution*, 33(3), 176–185.
- Drummond, A. J., Rambaut, A., Shapiro, B., & Pybus, O. G. (2005). Bayesian coalescent inference of past population dynamics from molecular sequences. *Molecular Biology and Evolution*, 22(5), 1185–1192.
- Dussex, N., Alberti, F., Heino, M. T., Olsen, R.-A., van der Valk, T., Ryman, N., Laikre, L., Ahlgren, H., Askeyev, I. V., Askeyev, O. V., Shaymuratova, D. N., Askeyev, A. O., Döppes, D., Friedrich, R., Lindauer, S., Rosendahl, W., Aspi, J., Hofreiter, M., Lidén, K., ... Díez-Del-Molino, D. (2020). Moose genomes reveal past glacial demography and the origin of modern lineages. *BMC Genomics*, 21(1), 854.
- Dussex, N., Tørresen, O. K., van der Valk, T., Le Moullec, M., Veiberg, V., Tooming-Klunderud, A., Skage, M., Garmann-Aarhus, B., Wood, J., Rasmussen, J. A., Pedersen, Å. Ø., Martin, S. L. F., Røed, K. H., Jakobsen, K. S., Dalén, L., Hansen, B. B., & Martin, M. D. (2023). Adaptation to the high-Arctic Island environment despite long-term reduced genetic variation in Svalbard reindeer. *iScience*, 26(10), 107811.
- Evanno, G., Regnaut, S., & Goudet, J. (2005). Detecting the number of clusters of individuals using the software STRUCTURE: A simulation study. *Molecular Ecology*, 14(8), 2611–2620.
- Fay, J. C., & Wu, C. I. (2000). Hitchhiking under positive Darwinian selection. *Genetics*, 155(3), 1405–1413.
- Festa-Bianchet, M., Ray, J. C., Boutin, S., Côté, S. D., & Gunn, A. (2011). Conservation of caribou (*Rangifer tarandus*) in Canada: An uncertain future. *Canadian Journal of Zoology*, 89(5), 419–434.

- Flagstad, Ø., Kvalnes, T., Røed, K. H., Våge, J., Strand, O., & Sæther, B.-E. (2022). *Genetisk levedyktig villreinbestand på Hardangervidda* (2176). Norsk Institutt for Naturforskning. <https://brage.nina.no/nina-xmlui/handle/11250/3020843>
- Frankham, R. (2005). Genetics and extinction. *Biological Conservation*, 126(2), 131–140.
- Frankham, R., Ballou, S. E. J., Briscoe, D. A., & Ballou, J. D. (2002). *Introduction to conservation genetics*. Cambridge University Press.
- Garcia-Erill, G., & Albrechtsen, A. (2020). Evaluation of model fit of inferred admixture proportions. *Molecular Ecology Resources*, 20(4), 936–949.
- Gravlund, P., Meldgaard, M., Pääbo, S., & Arctander, P. (1998). Polyphyletic origin of the small-bodied, high-arctic subspecies of tundra reindeer (*Rangifer tarandus*). *Molecular Phylogenetics and Evolution*, 10(2), 151–159.
- Grossen, C., Biebach, I., Angelone-Alasaad, S., Keller, L. F., & Croll, D. (2018). Population genomics analyses of European ibex species show lower diversity and higher inbreeding in reintroduced populations. *Evolutionary Applications*, 11(2), 123–139.
- Grossen, C., Guillaume, F., Keller, L. F., & Croll, D. (2020). Purging of highly deleterious mutations through severe bottlenecks in Alpine ibex. *Nature Communications*, 11(1), 1001.
- Hansen, B. B., Aanes, R., Herfindal, I., Kohler, J., & Saether, B.-E. (2011). Climate, icing, and wild arctic reindeer: Past relationships and future prospects. *Ecology*, 92(10), 1917–1923.
- Hansen, B. B., Pedersen, Å. Ø., Peeters, B., Le Moullec, M., Albon, S. D., Herfindal, I., Sæther, B., Grøtan, V., & Aanes, R. (2019). Spatial heterogeneity in climate change effects decouples the long-term dynamics of wild reindeer populations in the high Arctic. *Global Change Biology*, 25, 3656–3668.
- Heckeberg, N., & Wörheide, G. (2019). A comprehensive approach towards the systematics of Cervidae. <https://doi.org/10.7287/peerj.preprints.27618>
- Hoel, A. (1916). Hvorfra er Spitsbergenrenen kommet? *Naturen*.
- Isaksen, K., Nordli, Ø., Ivanov, B., Køltzow, M. A. Ø., Aaboe, S., Gjelten, H. M., Mezghani, A., Eastwood, S., Førland, E., Benestad, R. E., Hanssen-Bauer, I., Brækkan, R., Sviashchennikov, P., Demin, V., Revina, A., & Karandasheva, T. (2022). Exceptional warming over the Barents area. *Scientific Reports*, 12(1), 9371.
- IUCN. (2020). The IUCN red list of threatened species. Version 2020-1. *IUCN Red List of Threatened Species* (2020).
- Jensen, E. L., Díez-Del-Molino, D., Gilbert, M. T. P., Bertola, L. D., Borges, F., Cubric-Curik, V., de Navascués, M., Frandsen, P., Heuertz, M., Hvilsted, C., Jiménez-Mena, B., Miettinen, A., Moest, M., Pečnerová, P., Barnes, I., & Vernesi, C. (2022). Ancient and historical DNA in conservation policy. *Trends in Ecology & Evolution*, 37(5), 420–429.
- Johansen, B. E., Karlsen, S. R., & Tømmervik, H. (2012). Vegetation mapping of Svalbard utilising Landsat TM/ETM+ data. *The Polar Record*, 48(1), 47–63.
- Jónsson, H., Ginolhac, A., Schubert, M., Johnson, P. L. F., & Orlando, L. (2013). mapDamage2.0: Fast approximate Bayesian estimates of ancient DNA damage parameters. *Bioinformatics*, 29(13), 1682–1684.
- Kim, J., & Harismendy, O. (2017). *jihoonkim/DataMed-Admixture: bioCAD-DIE DataMed Admixture* (v1.0.4) (Version 1.0.4). <https://doi.org/10.5281/zenodo.1119073>
- Kircher, M., Sawyer, S., & Meyer, M. (2012). Double indexing overcomes inaccuracies in multiplex sequencing on the Illumina platform. *Nucleic Acids Research*, 40(1), e3.
- Kohn, M. H., Murphy, W. J., Ostrander, E. A., & Wayne, R. K. (2006). Genomics and conservation genetics. *Trends in Ecology & Evolution*, 21(11), 629–637.
- Korneliussen, T. S., Albrechtsen, A., & Nielsen, R. (2014). ANGSD: Analysis of next generation sequencing data. *BMC Bioinformatics*, 15, 356.
- Kumar, S., & Subramanian, S. (2002). Mutation rates in mammalian genomes. *Proceedings of the National Academy of Sciences of the United States of America*, 99(2), 803–808.
- Kvie, K. S., Heggernes, J., Anderson, D. G., Kholodova, M. V., Sipko, T., Mizin, I., & Røed, K. H. (2016). Colonizing the high arctic: Mitochondrial DNA reveals common origin of Eurasian archipelagic reindeer (*Rangifer tarandus*). *PLoS One*, 11(11), 1–15.
- Laikre, L., Allendorf, F. W., Aroner, L. C., Baker, C. S., Gregovich, D. P., Hansen, M. M., Jackson, J. A., Kendall, K. C., McKelvey, K., Neel, M. C., Olivieri, I., Ryman, N., Schwartz, M. K., Bull, R. S., Stetz, J. B., Tallmon, D. A., Taylor, B. L., Vojta, C. D., Waller, D. M., & Waples, R. S. (2010). Neglect of genetic diversity in implementation of the convention of biological diversity. *Conservation Biology: The Journal of the Society for Conservation Biology*, 24(1), 86–88.
- Lande, R., Engen, S., & Sæther, B.-E. (2003). *Stochastic population dynamics in ecology and conservation*. Oxford University Press.
- Le Moullec, M., Pedersen, Å. Ø., Stien, A., Rosvold, J., & Hansen, B. B. (2019). A century of conservation: The ongoing recovery of Svalbard reindeer. *The Journal of Wildlife Management*, 83(8), 1676–1686. <https://doi.org/10.1002/jwmg.21761>
- Leonardi, M., Librado, P., Der Sarkissian, C., Schubert, M., Alfarhan, A. H., Alquraishi, S. A., Al-Rasheid, K. A. S., Gamba, C., Willerslev, E., & Orlando, L. (2017). Evolutionary patterns and processes: Lessons from ancient DNA. *Systematic Biology*, 66(1), e1–e29.
- Li, H. (2013). Aligning sequence reads, clone sequences and assembly contigs with BWA-MEM. In *arXiv [q-bio.GN]*. arXiv. <http://arxiv.org/abs/1303.3997>
- Li, H., Handsaker, B., Wysoker, A., Fennell, T., Ruan, J., Homer, N., Marth, G., Abecasis, G., Durbin, R., & 1000 Genome Project Data Processing Subgroup. (2009). The sequence alignment/map format and SAMtools. *Bioinformatics*, 25(16), 2078–2079.
- Li, Z., Lin, Z., Ba, H., Chen, L., Yang, Y., Wang, K., Qiu, Q., Wang, W., & Li, G. (2017). Draft genome of the reindeer (*Rangifer tarandus*). *GigaScience*, 6(12), 1–5.
- Lin, Z., Chen, L., Chen, X., Zhong, Y., Yang, Y., Xia, W., Liu, C., Zhu, W., Wang, H., Yan, B., Yang, Y., Liu, X., Kvie, K. S., Røed, K. H., Wang, K., Xiao, W., Wei, H., Li, G., Heller, R., ... Li, Z. (2019). Biological adaptations in the Arctic cervid, the reindeer (*Rangifer tarandus*). *Science*, 364(6446), eaav6312. <https://doi.org/10.1126/science.aav6312>
- Loe, L. E., Liston, G. E., Pigeon, G., Barker, K., Horvitz, N., Stien, A., Forchhammer, M., Getz, W. M., Irvine, R. J., Lee, A., Movik, L. K., Mysterud, A., Pedersen, Å. Ø., Reinking, A. K., Ropstad, E., Trondrud, L. M., Tveraa, T., Veiberg, V., Hansen, B. B., & Albon, S. D. (2020). The neglected season: Warmer autumns counteract harsher winters and promote population growth in Arctic reindeer. *Global Change Biology*, 27, 993–1002. <https://doi.org/10.1111/gcb.15458>
- Lønø, O. (1959). *The reindeer on Svalbard* (report series no.83 in Norwegian). Norwegian Polar Institute. <https://brage.npolar.no/npolar-xmlui/bitstream/handle/11250/2395010/Meddelelser083.pdf?sequence=1>
- Lorenzen, E. D., Nogués-Bravo, D., Orlando, L., Weinstock, J., Binladen, J., Marske, K. A., Ugan, A., Borregaard, M. K., Gilbert, M. T. P., Nielsen, R., Ho, S. Y. W., Goebel, T., Graf, K. E., Byers, D., Stenderup, J. T., Rasmussen, M., Campos, P. F., Leonard, J. A., Koepfli, K.-P., ... Willerslev, E. (2011). Species-specific responses of late quaternary megafauna to climate and humans. *Nature*, 479(7373), 359–364.
- Luypaert, T., Hagan, J. G., McCarthy, M. L., & Poti, M. (2020). Status of marine biodiversity in the Anthropocene. In *YOUNMARES 9-the oceans: Our research, our future* (pp. 57–82). Springer.
- McKenna, A., Hanna, M., Banks, E., Sivachenko, A., Cibulskis, K., Kernytsky, A., Garimella, K., Altshuler, D., Gabriel, S., Daly, M., & DePristo, M. A. (2010). The genome analysis toolkit: A MapReduce

- framework for analyzing next-generation DNA sequencing data. *Genome Research*, 20(9), 1297–1303.
- Meisner, J., & Albrechtsen, A. (2018). Inferring population structure and admixture proportions in low-depth NGS data. *Genetics*, 210(2), 719–731.
- Mitchell, K. J., & Rawlence, N. J. (2021). Examining natural history through the lens of Palaeogenomics. *Trends in Ecology & Evolution*, 36(3), 258–267.
- Nei, M. (1987). *Molecular evolutionary genetics*. Columbia University Press.
- Nei, M., & Tajima, F. (1981). DNA polymorphism detectable by restriction endonucleases. *Genetics*, 97(1), 145–163.
- Nielsen, R., Korneliussen, T., Albrechtsen, A., Li, Y., & Wang, J. (2012). SNP calling, genotype calling, and sample allele frequency estimation from new-generation sequencing data. *PLoS One*, 7(7), e37558.
- Paradis, E. (2010). pegas: An R package for population genetics with an integrated-modular approach. *Bioinformatics*, 26(3), 419–420.
- Paradis, E., & Schliep, K. (2019). ape 5.0: An environment for modern phylogenetics and evolutionary analyses in R. *Bioinformatics*, 35(3), 526–528.
- Pečnerová, P., Lord, E., Garcia-Erill, G., Haghøj, K., Rasmussen, M. S., Meisner, J., Liu, X., van der Valk, T., Santander, C. G., Quinn, L., Lin, L., Liu, S., Carøe, C., Dalerum, F., Götherström, A., Måsviken, J., Vartanyan, S., Raundrup, K., Al-Chaer, A., ... Siegismund, H. R. (2023). Population genomics of the muskox' resilience in the near absence of genetic variation. *Molecular Ecology*, 32(2), e17205. <https://doi.org/10.1111/mec.17205>
- Peeters, B., Le Moullec, M., Raeymaekers, J. A. M., Marquez, J. F., Røed, K. H., Pedersen, Å. Ø., Veiberg, V., Loe, L. E., & Hansen, B. B. (2020). Sea ice loss increases genetic isolation in a high Arctic ungulate metapopulation. *Global Change Biology*, 26(4), 2028–2041.
- Peeters, B., Pedersen, Å. Ø., Loe, L. E., Isaksen, K., Veiberg, V., Stien, A., Kohler, J., Gallet, J.-C., Aanes, R., & Hansen, B. B. (2019). Spatiotemporal patterns of rain-on-snow and basal ice in high Arctic Svalbard: Detection of a climate-cryosphere regime shift. *Environmental Research Letters*, 14(1), 015002.
- Picard toolkit. (2019). Broad institute, GitHub repository. Broad Institute. <http://broadinstitute.github.io/picard/>
- Puechmaille, S. J. (2016). The program structure does not reliably recover the correct population structure when sampling is uneven: Subsampling and new estimators alleviate the problem. *Molecular Ecology Resources*, 16(3), 608–627.
- Quinlan, A. R. (2014). BEDTools: The Swiss-army tool for genome feature analysis. *Current Protocols in Bioinformatics/Editorial Board, Andreas D. Baxevanis ... [et Al.]*, 47, 11.12.1–11.12.34.
- R Core Team. (2021). R: A language and environment for statistical computing. R Foundation for Statistical Computing. <https://www.R-project.org/>
- Reimer, P. J. (2020). Composition and consequences of the IntCal20 radiocarbon calibration curve. *Quaternary Research*, 96, 22–27.
- Reimers, E. (1984). Body composition and population regulation of Svalbard reindeer. *Rangelands*, 4(2), 16–21.
- Robin, M., Ferrari, G., Akgül, G., Münger, X., von Seth, J., Schuenemann, V. J., Dalén, L., & Grossen, C. (2022). Ancient mitochondrial and modern whole genomes unravel massive genetic diversity loss during near extinction of Alpine ibex. *Molecular Ecology*, 31(13), 3548–3565.
- Rohland, N., & Reich, D. (2012). Cost-effective, high-throughput DNA sequencing libraries for multiplexed target capture. *Genome Research*, 22(5), 939–946.
- Sánchez-Barreiro, F., Gopalakrishnan, S., Ramos-Madrigal, J., Westbury, M. V., de Manuel, M., Margaryan, A., Ciucani, M. M., Vieira, F. G., Patramanis, Y., Kalthoff, D. C., Timmons, Z., Sicheritz-Pontén, T., Dalén, L., Ryder, O. A., Zhang, G., Marquès-Bonet, T., Moodley, Y., & Gilbert, M. T. P. (2021). Historical population declines prompted significant genomic erosion in the northern and southern white rhinoceros (*Ceratotherium simum*). *Molecular Ecology*, 30(23), 6355–6369.
- Schubert, M., Ermini, L., Der Sarkissian, C., Jónsson, H., Ginolhac, A., Schaefer, R., Martin, M. D., Fernández, R., Kircher, M., McCue, M., Willerslev, E., & Orlando, L. (2014). Characterization of ancient and modern genomes by SNP detection and phylogenomic and metagenomic analysis using PALEOMIX. *Nature Protocols*, 9(5), 1056–1082.
- Skotte, L., Korneliussen, T. S., & Albrechtsen, A. (2013). Estimating individual admixture proportions from next generation sequencing data. *Genetics*, 195(3), 693–702.
- Spielman, D., Brook, B. W., & Frankham, R. (2004). Most species are not driven to extinction before genetic factors impact them. *Proceedings of the National Academy of Sciences of the United States of America*, 101(42), 15261–15264.
- Stempniewicz, L., Kulaszewicz, I., & Aars, J. (2021). Yes, they can: Polar bears *Ursus maritimus* successfully hunt Svalbard reindeer *Rangifer tarandus platyrhynchus*. *Polar Biology*, 44(11), 2199–2206.
- Taylor, R. S., Horn, R. L., Zhang, X., Golding, G. B., Manseau, M., & Wilson, P. J. (2019). The Caribou (*Rangifer tarandus*) genome. *Genes*, 10(7), 540.
- Templeton, A. R., Crandall, K. A., & Sing, C. F. (1992). A cladistic analysis of phenotypic associations with haplotypes inferred from restriction endonuclease mapping and DNA sequence data. III. Cladogram estimation. *Genetics*, 132(2), 619–633.
- Therkildsen, N. O., Wilder, A. P., Conover, D. O., Munch, S. B., Baumann, H., & Palumbi, S. R. (2019). Contrasting genomic shifts underlie parallel phenotypic evolution in response to fishing. *Science*, 365(6452), 487–490.
- Trondrud, L. M., Pigeon, G., Król, E., Albon, S., Evans, A. L., Arnold, W., Hamby, C., Irvine, R. J., Ropstad, E., Stien, A., Veiberg, V., Speakman, J. R., & Loe, L. E. (2021). Fat storage influences fasting endurance more than body size in an ungulate. *Functional Ecology*, 35(7), 1470–1480.
- UniProt Consortium. (2021). UniProt: The universal protein knowledgebase in 2021. *Nucleic Acids Research*, 49(D1), D480–D489.
- van der Bilt, W. G. M., D'Andrea, W. J., Werner, J. P., & Bakke, J. (2019). Early Holocene temperature oscillations exceed amplitude of observed and projected warming in Svalbard lakes. *Geophysical Research Letters*, 46(24), 14732–14741.
- van der Knaap, W. O. (1989). Past vegetation and reindeer on Edgeoya (Spitsbergen) between c. 7900 and c. 3800 BP, studied by means of peat layers and reindeer Faecal pellets. *Journal of Biogeography*, 16(4), 379–394.
- van der Valk, T., Díez-Del-Molino, D., Marques-Bonet, T., Guschanski, K., & Dalén, L. (2019). Historical genomes reveal the genomic consequences of recent population decline in eastern gorillas. *Current Biology*, 29(1), 165–170.e6.
- van Oort, B. E. H., Tyler, N. J. C., Gerkema, M. P., Folkow, L., Blix, A. S., & Stokkan, K.-A. (2005). Circadian organization in reindeer. *Nature*, 438(7071), 1095–1096.
- Watterson, G. A. (1975). On the number of segregating sites in genetical models without recombination. *Theoretical Population Biology*, 7(2), 256–276.
- Werner, K., Müller, J., Husum, K., Spielhagen, R. F., Kandiano, E. S., & Polyak, L. (2016). Holocene sea subsurface and surface water masses in the Fram Strait – Comparisons of temperature and sea-ice reconstructions. *Quaternary Science Reviews*, 147, 194–209.
- Williamsen, L., Pigeon, G., Mysterud, A., Stien, A., Forchhammer, M., & Loe, L. E. (2019). Keeping cool in the warming Arctic: Thermoregulatory behaviour by Svalbard reindeer (*Rangifer tarandus platyrhynchus*). *Canadian Journal of Zoology*, 97(12), 1177–1185.
- Wollebaek, A. (1926). The Spitsbergen Reindeer: (*rangifer Tarandus Spetsbergensis*). *Dybwid*.

Yannic, G., Pellissier, L., Ortego, J., Lecomte, N., Couturier, S., Cuyler, C., Dussault, C., Hundertmark, K. J., Irvine, R. J., Jenkins, D. A., Kolpashikov, L., Mager, K., Musiani, M., Parker, K. L., Røed, K. H., Sipko, T., Pórisson, S. G., Weckworth, B. V., Guisan, A., ... Côté, S. D. (2013). Genetic diversity in caribou linked to past and future climate change. *Nature Climate Change*, 4(2), 132–137.

## SUPPORTING INFORMATION

Additional supporting information can be found online in the Supporting Information section at the end of this article.

**How to cite this article:** Kellner, F. L., Le Moullec, M., Ellegaard, M. R., Rosvold, J., Peeters, B., Burnett, H. A., Pedersen, Å. Ø., Brealey, J. C., Dussex, N., Bieker, V. C., Hansen, B. B., & Martin, M. D. (2024). A palaeogenomic investigation of overharvest implications in an endemic wild reindeer subspecies. *Molecular Ecology*, 33, e17274. <https://doi.org/10.1111/mec.17274>